CHALMERS
UNIVERSITY OF TECHNOLOGY

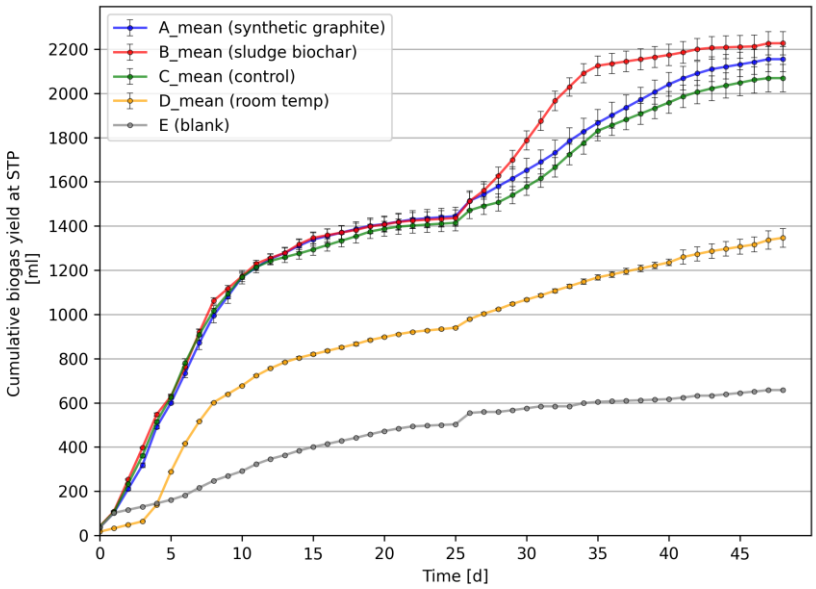

Effect of sludge biochar as an additive in thermophilic anaerobic digestion

Master's thesis in Infrastructure and Environmental Engineering

AASHUTOSH KUMAR THAKUR

DEPARTMENT OF ARCHITECTURE AND CIVIL ENGINEERING
CHALMERS UNIVERSITY OF TECHNOLOGY

Gothenburg, Sweden 2024
www.chalmers.se

MASTER'S THESIS ACEX30

Effect of sludge biochar as an additive in thermophilic anaerobic digestion

Master's Thesis in Infrastructure and Environmental Engineering

AASHUTOSH KUMAR THAKUR

Department of Architecture and Civil Engineering
Division of Water Environment Technology
CHALMERS UNIVERSITY OF TECHNOLOGY
Gothenburg, Sweden 2024

Effect of sludge biochar as an additive in thermophilic anaerobic digestion

Master's Thesis in Infrastructure and Environmental Engineering

AASHUTOSH KUMAR THAKUR

Master's thesis 2024: ACEX30

Supervisor: Oskar Modin
Examiner: Britt-Marie Wilen

Department of Architecture and Civil Engineering
Division of Water Environment Technology
Chalmers University of Technology
SE-412 96 Gothenburg
Sweden
Telephone: + 46 (0)31-772 1000

Cover image:
Upper left: Experimental setup showing anaerobic reactors inside an incubator
Lower left: Sewage sludge derived biochar used in the experiment
Right: Graph showing cumulative biogas yield in different reactor groups

Department of Architecture and Civil Engineering
Gothenburg, Sweden, 2024

Effect of sludge biochar as an additive in thermophilic anaerobic digestion

Master's thesis in Infrastructure and Environmental Engineering

AASHUTOSH KUMAR THAKUR

Department of Architecture and Civil Engineering
Division of Water Environment Technology
Chalmers University of Technology

ABSTRACT

The production of sewage sludge, the main byproduct of municipal wastewater treatment plants (WWTPs), is likely to increase due to growing urban populations and stricter effluent disposal regulations. Anaerobic digestion (AD) is among the most widely adopted methods in municipal WWTPs for the treatment and stabilisation of sewage sludge. The AD process has been found to perform optimally in two temperature regimes: mesophilic (35–40 °C) and thermophilic (55–60 °C), and it offers the advantage of recovering clean energy in the form of methane-rich biogas which can help offset the plant's energy costs.

Given the increasing constraints on energy supply, exploring ways to enhance biogas yield from AD becomes important. Sewage sludge pyrolysis is another technology that has received growing attention as an alternative method of sludge management. It involves heating the dewatered and dried sewage sludge at high temperatures (300–800 °C) in the absence of oxygen, producing sludge biochar as a byproduct. With properties that can favour microorganism growth and metabolism, sludge biochar could potentially improve anaerobic digestion performance when used as an additive during the digestion process.

This thesis investigates the impact of using sludge biochar as an additive in thermophilic anaerobic digestion of easily biodegradable substrates, specifically microcrystalline cellulose (MC) and sodium acetate (SA). A batch anaerobic digestion experiment was conducted over 49 days in two consecutive phases: the first phase using MC and the second phase using SA as substrates. Sludge biochar (SB) and synthetic graphite (SG) were used as additives in two different reactor groups to assess their impact on the cumulative biogas yield.

Results from Phase 1 showed that the overall biogas yield in the SB and SG dosed reactors exceeded the control group by 1.5% and 2.1% respectively, indicating a minimal impact of SB on thermophilic anaerobic digestion of MC. However, results from Phase 2 using SA as the substrate showed that biogas yield in the SB and SG dosed reactors exceeded the control by around 21% and 8.5% respectively, indicating a much greater impact of the additive. This suggests that SB could have influenced the methanogenesis reactions in the second phase, resulting in an increase in total biogas yield. While SB shows potential as an additive for improving anaerobic digestion performance, further investigations are needed to understand the enhancement mechanism and its potential application with sewage sludge digestion.

Keywords: wastewater treatment plant, sewage sludge, anaerobic digestion, sludge pyrolysis, biochar, sludge biochar, biogas, methanogenesis.

Table of contents

ACKNOWLEDGEMENTS

This thesis was written to fulfill the requirements of the Master's degree program in Infrastructure and Environmental Engineering at Chalmers University of Technology and was produced during my scholarship period funded by the Swedish Institute. The experimental work was carried out at the Water and Environment Lab at Chalmers between January and April 2024.

I extend my deepest gratitude to my supervisor, Oskar Modin, for his invaluable support, guidance, and encouragement. His expertise and insights were crucial for the successful completion of this project. I also sincerely thank my examiner, Britt-Marie Wilen, for her thoughtful guidance and constructive feedback, which greatly enhanced the quality of my work.

My heartfelt thanks go to Amir Saeid Mohammadi for his support and assistance with the laboratory work. Additionally, I am grateful to Dag Lorick from Gryaab AB for providing the digested sludge sample and for sharing his valuable knowledge and experience with me.

To my parents, thank you for your encouragement and unwavering belief in me. To my wife Anuja, thank you for your love and constant support, which have been my pillars of strength throughout this journey.

Aashutosh Kumar Thakur

Göteborg, June 2024

LIST OF ABBREVIATIONS

AD	Anaerobic Digestion
AM	Acetoclastic Methanogenesis
BC	Biochar
BMP	Biomethane Potential Test
DIET	Direct Interspecies Electron Transfer
EC	Electrical Conductivity
HM	Hydrogenotrophic Methanogenesis
ISR	Inoculum to Substrate Ratio
LCFA	Long Chain Fatty Acid
MAD	Mesophilic Anaerobic Digestion
OLR	Organic Loading Rate
PS	Primary Sludge
SAO	Syntrophic Acetate Oxidation
SAOB	Syntrophic Acetate Oxidising Bacteria
SB	Sludge Biochar
SG	Synthetic Graphite
SRT	Solids Retention Time
STP	Standard Temperature and Pressure
TAD	Thermophilic Anaerobic Digestion
TAN	Total Ammonia Nitrogen
TS	Total Solids
VFA	Volatile Fatty Acid
VS	Volatile Solids
WAS	Waste Activated Sludge
WWTP	Wastewater Treatment Plant

1 Introduction

Global wastewater production is projected to increase by 24% by 2030 and 51% by 2050 compared to current levels, underlining the growing importance of wastewater treatment plants (WWTPs) in keeping natural water bodies safe from pollution (Qadir et al., 2020). In line with this, one of the main targets of Sustainable Development Goal 6 is to halve the proportion of untreated wastewater discharged into natural water bodies by 2030, together with substantially increasing their recycling and safe reuse. This has spurred municipal WWTPs to improve and increase their existing treatment capacity to comply with the stricter effluent disposal regulations. This anticipated development in wastewater treatment will lead to a parallel increase in the production of sewage sludge – the main byproduct of WWTPs. In 2020, over 8.7 million tons of sewage sludge dry mass was produced in the European Union, while more than 200,000 tons was produced in Sweden alone (EurEau, 2021; Dagerskog & Olsson, 2020).

Sewage sludge produced in a conventional WWTP can be classified into two types - primary sludge (PS) which settles in the primary sedimentation tanks; and secondary sludge or waste activated sludge (WAS) which settles in the secondary sedimentation tank after the completion of biological treatment process (Gebreeyessus & Jenicek, 2016). PS primarily consists of suspended inorganic and organic solids, and is poor in microorganisms, whereas WAS is rich in bacterial flocs and microorganisms (Sun et al., 2021). The management of this sludge is challenging because of the large quantity produced and their high concentration of pathogens and heavy metals. As a result, sludge management constitutes a significant component of WWTPs, typically accounting for around 30% of the plant's initial capital cost and 50–60% of its operational cost (Gebreeyessus & Jenicek, 2016; Appels et al., 2008). A typical process layout of a conventional WWTP consisting of wastewater line, sludge line and reject water line is illustrated in Figure 1.1.

Anaerobic digestion (AD) is among the most widely adopted sludge stabilisation methods, especially adopted in larger municipal WWTPs, for its advantages like recovery of clean energy, reduction of sludge volume and destruction of pathogens (Gebreeyessus & Jenicek, 2016). AD consists of a complex process in which microorganisms break down the organic matter of sewage sludge through a series of biochemical reactions in an oxygen-free environment, producing a methane-rich biogas and a liquid residue rich in micro and macronutrients. The AD process has been found to perform optimally in two temperature regimes – mesophilic (35–40 °C) and thermophilic (55–60 °C). Mesophilic anaerobic digestion (MAD) has been the conventionally adopted method in majority of WWTPs because of its greater process stability and lower energy requirements. However, thermophilic anaerobic digestion (TAD) offers an interesting alternative to MAD as it results in a higher reduction of pathogens in the stabilised biosolids and has faster reaction rates giving increased biogas production, although at a cost of reduced process stability and higher energy demand (Labatut et al., 2014).

Another method of sludge management that has seen growing interest is sludge pyrolysis (Djandja et al., 2020; Agrafioti et al., 2013). Sludge pyrolysis involves the combustion of dried sewage sludge within a high temperature range of 300–800 °C in the absence of oxygen, resulting in the production of a carbon-rich, solid by-product known as biochar. Production of sludge biochar (SB) from sewage sludge can be a viable method of sustainable sludge management at WWTPs. Thermochemical conversion of sewage sludge into biochar can significantly reduce sludge volume

minimising its disposal costs, destroy pathogens and yield a versatile resource with various applications.

In Sweden, AD plants have been in use since the 1940s to reduce sludge quantities from wastewater treatment, and it later became a common practice during the great expansion of wastewater treatment in the 1960s (Gustafsson & Anderberg, 2023; SEPA, 2012). In 2011, there were 135 AD plants in operation for treatment of sewage sludge, producing 638 gigawatt-hours of clean energy per year (Persson, 2012). Today, the country aims to further increase its biogas output from anaerobic digestion from 2 terawatt-hours per year in 2020 to 7 terawatt-hours per year by 2030, in line with its national energy goals and European Union climate objectives (Gustafsson & Anderberg, 2023).

Conventional AD plants in Swedish WWTPs typically operate within the mesophilic temperature range of 35–40 °C, although operation at higher thermophilic temperatures of 55–60 °C is also possible. Research has also shown that using biochar as additives can improve digester performance by boosting microorganism metabolism, mitigating inhibitor stress, and promoting process stability (Zhang et al., 2019). Given these possibilities, WWTPs are increasingly interested in converting their mesophilic AD plants to high-temperature operation and exploring the use of additives such as sludge biochar to enhance biogas production.

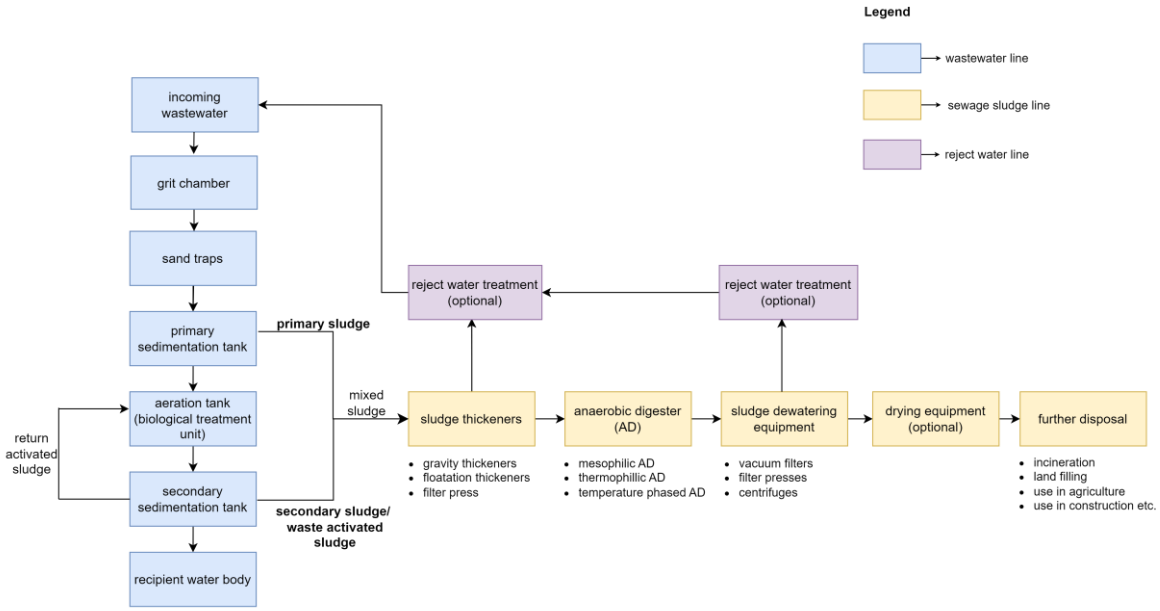

Figure 1.1 Process layout at a conventional WWTP (adapted from Lanko, 2021*).*

1.1 Aim

This master's thesis project aimed to investigate the effect of sludge biochar as an additive in thermophilic anaerobic digestion, examining its impact on biogas production. This was accomplished by performing a lab scale anaerobic digestion experiment using batch reactors fed with easily degradable substrates. The experiment was carried out in two consecutive phases, with the Phase 1 using microcrystalline cellulose and Phase 2 using sodium acetate as substrate.

The specific aims of this thesis included the following:

i. Design and conduct a laboratory-scale experiment to investigate daily biogas production in batch anaerobic reactors maintained at 55 °C and 21 °C, fed with easily biodegradable substrates and supplemented with and without sludge biochar as additives.

ii. Monitor and record daily biogas production in the batch reactors by measuring their headspace pressure and normalising it to biogas volume at standard temperature and pressure (STP).

iii. Analyse the recorded data and present results showing the biogas production curves in different reactor groups, comparing their digestion performance.

1.2 Limitations

The limitations of this thesis study include the following:

i. Given the limited timeframe for this study, the batch experiment was conducted using a single inoculum to substrate (ISR) ratio of 2, a substrate concentration of 10 g VS/l and an additive concentration of 50 g/l in the test reactors.

ii. The experiment used only one blank reactor to measure the background biogas production from the inoculum at 55 °C. There was no blank reactor for the reactor group at room temperature.

iii. The effect of vapour pressure on the measured headspace pressure was not considered. It was assumed that the pressure build up inside the reactors was solely due to the produced biogas consisting of methane and carbon dioxide.

2 Background

Anaerobic digestion is among the most widely adopted methods used for sludge stabilisation in municipal WWTPs. It is favoured over other sludge management alternatives due to its advantages like reduction of sludge volume by up to 50%, destruction of pathogens, removal of bad odour and recovery of clean energy in the form of biogas (Gebreeyessus & Jenicek, 2016). It is particularly favoured in larger WWTPs, with a capacity of over 20,000 population, where energy recovery from utilising the produced biogas becomes economically advantageous (Foladori et al., 2010).

2.1 Mechanism of anaerobic digestion process

The process of anaerobic digestion occurs through a series of biochemical reactions in which a consortium of microorganisms collaborate to break down complex organic polymers in multiple stages and convert them into a gaseous mixture consisting of methane (50–70%), carbon dioxide (30–50%) and trace levels of other gases like hydrogen sulphide, ammonia, nitrogen and hydrogen (Uddin & Wright, 2021). The process also produces a stable liquid digestate which is a mix of bacterial biomass and inert organics. At the start, anaerobic digesters are usually inoculated with a mixed microbial consortium from running digesters after which the microbial community develops over time depending upon the characteristics of inoculum, substrate and environmental growth conditions (Menzel et al., 2020). The biochemical reactions taking place during anaerobic digestion is completed in four stages: (i) hydrolysis (ii) acidogenesis (iii) acetogenesis and (iv) methanogenesis, which has been shown schematically in Figure 2.1. These biochemical reactions occur simultaneously in an oxygen-free environment and are directly linked in such a manner that the byproduct of one phase acts as the substrate for the next phase.

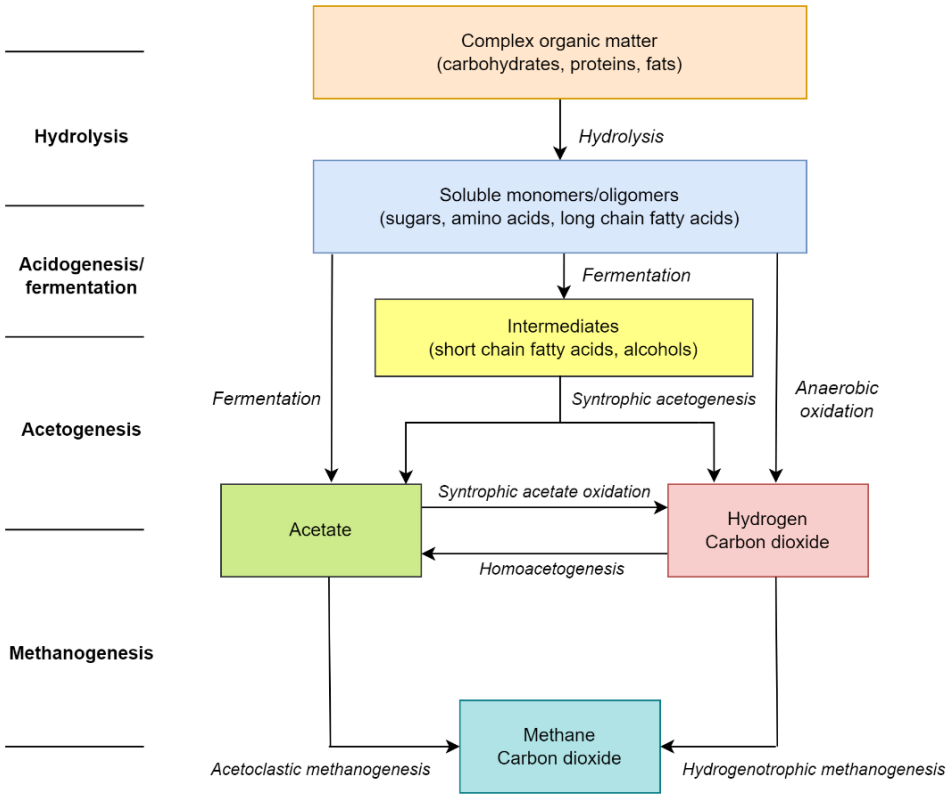

Figure 2.1 *Schematic representation of the different stages of anaerobic digestion (adapted from* Schnürer & Jarvis, 2018*).*

2.1.1 Hydrolysis

It is the first stage in anaerobic digestion process in which extracellular enzymes secreted by the microbial community break down complex organic molecules of proteins, carbohydrates and lipids into their respective simpler units of amino acids, monosaccharides and fatty acids (Schnürer & Jarvis, 2018). This biodegradation of higher mass organic molecules is very important as the resulting low weight intermediates can be absorbed and used by microorganisms as food source in subsequent stages. Hydrolysis is generally considered as the rate-limiting step as it depends upon the freely accessible surface area of the organic matter and overall structure of the solid substrate (Chen et al., 2020). Some products after hydrolysis are ready to be converted into biogas but most others need additional breakdown through subsequent stages. Equation 2.1 shows a typical hydrolysis reaction in which cellulose, a complex carbohydrate, is broken down into glucose, its monomer unit, due to the action of hydrolytic enzymes.

$$(C_6H_{10}O_5)_n + nH_2O \rightarrow nC_6H_{12}O_6 + nH_2 \qquad \text{[Equation 2.1]}$$

2.1.2 Acidogenesis

In the second stage of anaerobic digestion, which is also known as fermentation, the soluble organic monomers and oligomers formed after hydrolysis are further broken down by acidogenic bacteria into volatile fatty acids (VFAs) and alcohols along with

by-products like carbon dioxide, hydrogen, ammonia and acetates (Schnürer & Jarvis, 2018). The most common VFAs include acetic, propionic, isobutyric, butyric, isovaleric, valeric and caproic acids (Wainaina et al., 2019). The by-products carbon dioxide, hydrogen and acetates can readily be converted into methane after this stage but the produced VFAs and alcohols need further decomposition in the next stage. Acidogenesis is a fast process, but it involves the risk of VFA accumulation in the digester which can result in acidification of reactors that can cause process inhibition. Among the VFAs, the effect of propionic acid on system disruption is stronger than other acids (Schnürer & Jarvis, 2018). Nitrogen-rich substrates can also lead to increased production of ammonia which at high concentrations can inhibit the growth of microorganisms (Schnürer & Nordberg, 2008). Equation 2.2–2.4 illustrate typical acidogenic reactions on glucose producing ethanol, ethanoic acid and propionic acid, along with byproducts.

$$C_6H_{12}O_6 \leftrightarrow 2CH_3CH_2OH + 2CO_2 \quad \text{[Equation 2.2]}$$

$$C_6H_{12}O_6 + 2H_2 \leftrightarrow 2CH_3CH_2COOH + 2H_2O \quad \text{[Equation 2.3]}$$

$$C_6H_{12}O_6 \rightarrow 3CH_3COOH \quad \text{[Equation 2.4]}$$

2.1.3 Acetogenesis

This is the third stage during anaerobic digestion in which the produced VFAs and alcohols are further digested by acetogenic bacteria to produce hydrogen, carbon dioxide and acetic acid. Hydrogen plays a key role in this process since the acetogenic reaction is thermodynamically possible only if the partial hydrogen pressure in the digester is less than 10^{-4} atmospheric pressure (Uddin & Wright, 2021). This condition is made possible due to the syntrophic collaboration between two microbial groups, as the hydrogen produced by the acetogenic bacteria is used up by the hydrogenotrophic methanogens in the final stage to produce methane, lowering the partial hydrogen pressure in the system. Compared to other steps in anaerobic digestion, acetogenesis is believed to proceed at the fastest rate, but this is strongly dependent upon the rate of interspecies hydrogen transfer between the two microbial groups (Meegoda et al., 2018). Equation 2.5–2.7 shows acetogenic reactions producing acetate, carbon dioxide and hydrogen from the previously produced organic acids and alcohols.

$$CH_3CH_2COO^- + 3H_2O \leftrightarrow CH_3COO^- + H^+ + HCO_3^- + 3H_2 \quad \text{[Equation 2.5]}$$

$$C_6H_{12}O_6 + 2H_2O \leftrightarrow 2CH_3COOH + 2CO_2 + 4H_2 \quad \text{[Equation 2.6]}$$

$$CH_3CH_2OH + 2H_2O \leftrightarrow CH_3COO^- + 3H_2 + H^+ \quad \text{[Equation 2.7]}$$

2.1.4 Methanogenesis

In the final stage of anaerobic digestion, methanogenic archaea utilise the previously produced acetate, carbon dioxide and hydrogen to produce methane and carbon dioxide (Schnürer & Jarvis, 2018). Methane production occurs through two main methanogenesis pathways: acetoclastic methanogenesis, in which acetate-consuming

methanogens split acetate into methane and carbon dioxide (Equation 2.8), and hydrogenotrophic methanogenesis in which hydrogen-consuming methanogens reduce carbon dioxide into methane (Equation 2.9) (Uddin & Wright, 2021). A less prevalent third pathway also exists in which methylotrophic methanogens consume methyl compounds like methanol, methylamines and methyl sulphide to produce methane (Equation 2.10), but this constitutes a very small share of the produced methane (Conrad, 2020). Hydrogenotrophic methanogenesis plays a crucial role by consuming the previously produced hydrogen, and maintaining a low hydrogen pressure in the digester which enables the otherwise unfavourable acetogenic reactions to move forward. Methanogens are very sensitive to pH changes and have the slowest regeneration rates (5–16 days) among the microbial groups involved in anaerobic digestion process, making this the most sensitive and critical step (Meegoda et al., 2018).

$$CH_3COOH \rightarrow CH_4 + CO_2 \quad \text{[Equation 2.8]}$$

$$CO_2 + 4H_2 \rightarrow CH_4 + 2H_2O \quad \text{[Equation 2.9]}$$

$$CH_3OH + H_2 \rightarrow CH_4 + H_2O \quad \text{[Equation 2.10]}$$

2.2 Microorganisms in anaerobic digestion process

The majority of microorganisms involved in anaerobic digestion belong to the domain *Bacteria*, except for methane producers, which exclusively belong to the domain *Archaea* (Schnürer & Jarvis, 2018). Among the bacteria, the most common phyla include *Firmicutes, Bacteroidetes, Proteobacteria, Synergistetes, Chloroflexi, Fibrobacteres, Spirochaetes, Planctomycetes, Tenericutes, Verrucomicrobia, Acidiobacteria* and *Actinobacteria*. Among these, *Bacteroidetes, Firmicutes, Chloroflexi*, and *Proteobacteria* are particularly abundant, housing most of the known species of hydrolytic and acidogenic bacteria (Schnürer & Jarvis, 2018). Hydrolytic bacteria secrete extracellular enzymes to break down organic compounds. They exhibit fast growth rates and are relatively resilient to shifts in environmental conditions like pH and temperature. Acidogenic bacteria then further metabolise the products of hydrolysis, converting them into VFAs, alcohols, ammonia, and carbon dioxide through fermentation reactions.

The acetogenic bacteria are diverse but are primarily classified within the phylum *Firmicutes* (Schnürer & Jarvis, 2018). They are strict anaerobes and are considered quite sensitive to the changes in the process environment as compared to other bacteria. Their main role involves converting products from the acidogenic phase into acetic acid, carbon dioxide, and hydrogen, which serve as key substrates for methanogens. They also play an important role in the degradation of propionate, butyrate and other VFAs which is crucial for maintaining the stability of the digestion process. Common acetogens involved in these processes include *Pelotomaculum, Smithella, Syntrophobacter, Syntrophus* and *Syntrophomonas* (Harirchi et al., 2022). There also exists a syntrophic association between the syntrophic acetate-oxidising bacteria (SAOB) and the hydrogenotrophic methanogens, in which the methanogens utilise the hydrogen produced by the SAOB to produce methane, thereby lowering the reactor's partial hydrogen pressure and enabling acetogenesis (Harirchi et al., 2022). SAOB involved in this process consist of both thermophillic and mesophillic species, including

Thermacetogenium phaeum, Thermotoga lettingae, Syntrophaceticus schinkii, Tepidanaerobacter acetatoxydans and *Clostridium ultunense* (Mosbaek et al., 2016).

The methanogenic archaea are unique for their methane-producing ability and extreme sensitivity to oxygen, setting them apart from other species. Although less abundant than bacteria, they mainly belong to the phylum *Euryarchaeota* (Schnürer & Jarvis, 2018). Methanogens are categorized into three main groups based on their methanogenesis pathways: acetoclastic methanogens, which use acetate to produce methane and carbon dioxide; hydrogenotrophic methanogens, which use hydrogen to convert carbon dioxide into methane; and methylotrophic methanogens which produce methane from demethylation of compounds containing methyl group (Deublein & Steinhauser, 2008; Conrad, 2020). Acetoclastic methanogens fall into two genera: *Methanosarcina* and *Methanothrix* (formerly *Methanosaeta*). *Methanosarcina* is a facultative acetoclastic methanogen and can utilise both methanogenesis pathways. It has a higher growth rate and shows a lower affinity for acetate. *Methanothrix*, on the other hand, solely utilizes acetate for methane production and can thrive even at low acetate concentrations despite having a slower growth rate. Common hydrogenotrophic methanogens include *Methanobacterium, Methanobrevibacter, Methanoculleus, Methanospirillum,* and *Methanothermobacter* (Harirchi et al., 2022).

2.2.1 Microbial metabolism pathways

Microorganisms use different metabolic strategies to carry out their specific roles in the different stages of anaerobic digestion. These microorganisms need a carbon source to build and repair their cells, an energy source for running their cellular processes and a means of transferring electrons from one compound to another (Plante et al., 2015). Carbon sources can be either organic (carbohydrates, fats, and proteins) or inorganic (such as carbon dioxide), as shown in Table 2.1. For energy, they rely exclusively on chemical energy which can come from inorganic compounds like hydrogen or from organic compounds like sugars, fats, or proteins (Plante et al., 2015). This acquisition of chemical energy is achieved through oxidation-reduction reactions in which electrons are exchanged between donors and acceptors.

Table 2.1 Carbon sources, energy sources and terminal electron receptors for microorganisms involved in anaerobic digestion.

Carbon source	**Energy source**	**Terminal electron receptor**
CO_2 *(autotrophy)*	Inorganic compounds: H_2 *(lithotrophy)*	O_2 *(aerobic respiration)*
Organic compounds *(heterotrophy)*	Organic compounds: sugar, fat, protein *(organotrophy)*	$NO_3^-, Mn^{4+}, Fe^{3+}\ SO_4^{-2}, CO_2$ *(anaerobic respiration)*
		Organic compounds *(fermentation)*

The molecule that undergoes reduction upon receiving electrons at the end of the electron transport chain is known as the terminal electron acceptor. In case of aerobic respiration, oxygen (O_2) serves as the terminal electron acceptor. When there is no

oxygen, either anaerobic respiration or fermentation occurs. Anaerobic respiration occurs when the terminal electron acceptor is an inorganic compound such as nitrate (NO_3^-), manganese (Mn^{4+}), iron (Fe^{3+}), sulphate (SO_4^{-2}), or carbon dioxide (CO_2). Conversely, fermentation occurs when the terminal electron acceptor is organic, resulting in the production of acids, alcohols, hydrogen gas, and carbon dioxide. The reduction of electron acceptors yields varying amounts of energy to the microorganisms, with O_2 providing the most energy and CO_2 the least (Plante et al., 2015). In aerobic processes, microorganisms utilize surplus energy to produce a significant amount of biomass, while in anaerobic processes, up to 90% of substrate energy remains bound to the biogas (Koch et al., 2020). CO_2 abundance in anaerobic digesters favours the methanogens that use CO_2 as an electron acceptor. However, the presence of other electron acceptors can reduce methane production as methanogens may be outcompeted by other microorganisms utilizing the same substrate.

2.2.2 Methanogenesis pathways

As discussed in Section 2.1.4, methane can be produced during AD by three groups of methanogens: acetoclastic methanogens, hydrogenotrophic methanogens and methylotrophic methanogens. Based on the main substrate used for methanogenesis, there are three main methanogenesis pathways: (i) pathway using acetate (ii) pathway using H_2/CO_2 (iii) pathway using methyl compounds (Conrad, 2020). The first two pathways are the major pathways producing the bulk share of methane, while the pathway using methyl compounds produces only a small share of methane during anaerobic digestion.

The first pathway using acetate can proceed either through acetoclastic methanogenesis (AM), in which acetate consuming methanogens directly split the acetate into methane (Equation 2.11) and carbon dioxide, or through the two-step syntrophic acetate oxidation (SAO) followed by hydrogenotrophic methanogenesis (HM), in which syntrophic acetate oxidising bacteria (SAOB) first convert the acetate into hydrogen and carbon dioxide, which is then utilised by hydrogenotrophic methanogens to reduce carbon dioxide into methane (Equation 2.12 and 2.13) (Dyksma et al., 2020). The overall reaction for both AM and SAO-HM pathways have the same stoichiometry; having an overall Gibbs free energy of -31 kJ/mole in both cases. However, the energy produced in the SAO-HM pathway needs to be shared by two microorganisms that have to struggle close to the thermodynamic equilibrium, making AM the favoured pathway in mesophilic conditions.

HM is the second pathway in which carbon dioxide is reduced to methane by hydrogen consuming methanogens. Apart from hydrogen, the reduction of carbon dioxide can also occur in presence of formate or simple alcohols. In HM, the balance between hydrogen pressure in the digester and the inter-species hydrogen transfer between acetogens and hydrogenotrophic methanogens plays a crucial role in keeping the digestion process stable. Excessive hydrogen concentration inhibits acetogenesis whereas too low hydrogen hinders methane production by hydrogenotrophic methanogens. Thermodynamically, hydrogenotrophic methanogenesis has a higher Gibbs free energy of -135.6 kJ/mol, making it less favourable than AM at normal operating conditions.

The primary methanogenesis pathway during anaerobic digestion has been observed to be influenced by parameters such as process temperature and ammonia concentration

(Dyksma et al., 2020; Yang et al., 2018). In municipal anaerobic digesters operated at mesophilic temperatures, AM has been observed to be the dominant pathway, producing over two-thirds of the total methane with the rest coming from hydrogenotrophic methanogenesis (Schnürer & Jarvis, 2018). However, at thermophilic temperatures, it has been observed that the acetoclastic methanogens are outcompeted by the SAOB, bringing a shift in the dominant methanogenesis pathway (Schnürer & Nordberg, 2008). This shift may occur because syntrophic acetate oxidation becomes thermodynamically more favourable at higher temperatures. Furthermore, the thermophilic degradation of nitrogen-rich substrates like sewage sludge leads to increased ammonia production. This increased ammonia concentration has been found to have a greater inhibitory effect on the acetoclastic methanogens compared to hydrogenotrophic methanogens (Schnürer & Nordberg, 2008). As a result, under such high ammonia conditions, SAO-HM can become the dominant process for acetate consumption, bringing a shift in the dominant methanogenesis pathway.

$$CH_3COO^- + H_2O \rightarrow CH_4 + HCO_3^- \qquad (\Delta G^{0'} = -31.0 \text{ kJ mol}^{-1})$$

[Equation 2.11]

$$CH_3COO^- + 4H_2O \rightarrow 2HCO_3^- + 4H_2 + H^+ \qquad (\Delta G^{0'} = +104.6 \text{ kJ mol}^{-1})$$

[Equation 2.12]

$$4H_2 + HCO_3^- + H^+ \rightarrow CH_4 + 3H_2O \qquad (\Delta G^{0'} = -135.6 \text{ kJ mol}^{-1})$$

[Equation 2.13]

2.3 Factors influencing anaerobic digestion performance

Various operational parameters influence the performance of anaerobic digestion, impacting biogas yield, pathogen destruction, sludge volume reduction, and process stability. These parameters, which are numerous and depend on factors such as feedstock, process conditions, process inhibitions, reactor design and reactor control, have been listed in Table 2.2 (Deublein & Steinhauser, 2008; Sarker et al., 2019). While discussing all these parameters exceeds the scope of this thesis project, this section briefly addresses crucial factors like substrate composition, carbon-to-nitrogen ratio, pH, VFA accumulation and ammonia inhibition. Detailed discussions on the effect of temperature and use of biochar as additives are provided in Sections 2.5 and 2.6, respectively.

Table 2.2 Parameters affecting anaerobic digestion performance.

1. Feedstock	▪ Substrate composition ▪ Carbon to nitrogen ratio (C:N ratio) ▪ Inoculum ▪ Co-digestion ▪ Pre-treatment ▪ Use of additives
2. Process condition	▪ Temperature ▪ pH
3. Reactor design	▪ Batch versus continuous ▪ Feedstock water content (wet versus dry) ▪ Mixing versus no mixing
4. Reactor control	▪ Hydraulic retention time (HRT) ▪ Organic loading rate (OLR)
5. Process inhibition	▪ VFA accumulation ▪ Ammonia inhibition

Substrate composition: The quantity of biogas produced has been found to be influenced by the physical and chemical characteristics of the substrate, which primarily constitutes of carbohydrates, lipids, and proteins. Lipids have been identified as having the highest potential for methane production, although their breakdown into long-chain fatty acids (LCFAs) can also hinder the digestion process (Holohan et al., 2022). Additionally, waste materials rich in proteins and fats, such as municipal solid waste, food waste, fish waste, and sewage sludge, can lead to production of ammonia and sulphides, potentially disrupting the digestion process (Rajagopal et al., 2013).

C:N ratio: The ratio of carbon to nitrogen in the substrate is another crucial factor in the digestion process. Microorganisms rely on carbon for energy and require nitrogen for growth and metabolism. Maintaining an optimal C:N ratio ensures a balanced nutritional environment for the microbes and promotes stable pH levels throughout digestion. Theoretically, the most efficient methane production occurs when the C:N ratio falls between 25 to 30:1, depending on the specific characteristics of the substrate (Gaur & Bardiya, 1997). Higher ratios can deplete nitrogen rapidly, hindering methane production and reducing overall biogas output. Conversely, lower ratios may lead to excessive ammonia production, causing pH levels to rise and biogas yield to fall (Muzenda, 2014).

pH: Even though anaerobic digestion has been found to be feasible within a pH range of 5.5–8.5, methanogens, which are the most sensitive microbial group in the digestion process, operate optimally at a pH of around 7 (Schnürer & Jarvis, 2018). Even minor pH changes can have a profound impact on their microbial metabolism, affecting reaction rates and methane production. Failure to metabolize intermediates produced during digestion, like VFAs and ammonia, can lead to a significant decrease in pH levels, potentially causing process inhibition or failure. Achieving an ideal pH level for all microorganisms within a single digester can be challenging, especially when digesting substrates with varying compositions, such as sewage sludge.

VFA accumulation: VFAs are among the main intermediate products formed during the acidogenesis phase of AD, consisting mainly of acetic, propionic, isobutyric, butyric, isovaleric, valeric and caproic acids (Schnürer & Jarvis, 2018). These VFAs are largely transformed into acetate, which is subsequently converted to methane through methanogenesis. Efficient VFA conversion is advantageous for maintaining a balanced pH and achieving improved methane production. However, achieving optimal VFA conversion during digestion may be challenging due to variations in organic loading rate, pH, temperature, and partial hydrogen pressure, potentially leading to VFA accumulation and process inhibition.

Ammonia inhibition: Ammonia is produced during the decomposition of nitrogen-rich materials in the feedstock. In digesters, the main inorganic forms of ammonia nitrogen are free ammonia (NH_3) and ammonium ion (NH_4^+), with free ammonia having a greater inhibitory effect on microorganisms. Most of the ammonia is usually produced during hydrolysis stage, and the type produced is influenced by factors such as temperature, pH, inoculum or microbial community (Sarker et al., 2019).

2.4 Impact of temperature on anaerobic digestion

Temperature plays a crucial role in the anaerobic digestion process, impacting both physiochemical parameters and microbiota. Anaerobic digesters are most typically operated at mesophilic (35–40 °C) or thermophilic (50–55 °C) temperature regimes (Metcalf & Eddy, 2014). These two temperature modes are considered optimal for process stability, biogas production, and microbial adaptability. Mesophilic anaerobic digestion (MAD) has been widely adopted in municipal WWTPs due to its good process stability and lower energy requirement. On the other hand, adoption of thermophilic anaerobic digestion (TAD) has been limited due to its higher energy demand and poor stability. However, TAD has been gaining favour in recent times due to its advantages of having faster biogas production rates, higher sludge degradation rates and better inactivation of pathogens (Gebreeyessus & Jenicek, 2016).

Among the microorganisms involved in the digestion process, methanogens are the most sensitive group to temperature changes (Schnürer & Jarvis, 2018). In case of temperature change, methanogens stop producing methane while the more resilient acidogenic and acetogenic bacteria continue producing VFAs and alcohols. These products are then not digested by the inactive methanogens resulting in acid accumulation. In the absence of a good buffering capacity, the pH can drop significantly inhibiting the digestion process altogether. Hence, it is important to have a steady temperature in the digestion tank which is often achieved by some form of mixing and having good thermal insulation.

2.4.1 Thermophilic versus mesophilic anaerobic digestion

The higher temperature in TAD accelerates substrate degradation, resulting in higher methane production compared to MAD (Schnürer & Jarvis, 2018). This increased methane yield can offset the higher energy demand required to maintain the elevated temperature. Moreover, the faster reaction rates in TAD lead to more rapid substrate breakdown, potentially reducing digester volume. The higher temperature in TAD also gives better pathogen removal capabilities, making it more widely acceptable for meeting the sludge discharge limits set by environmental regulatory agencies.

However, TAD is more sensitive to disturbances making the process less stable. This could be because thermophilic microorganisms are more temperature sensitive and even small changes in temperature can cause process disturbances because of imbalance between fermentation and methane production. In case of nitrogen rich substrates like sewage sludge, the higher temperature and faster degradation rate can also result in faster ammonia production, potentially leading to ammonia inhibition if not addressed. Furthermore, compared to MAD, TAD exhibits lower microbial diversity despite faster reaction rates, which may contribute to its reduced stability since greater microbial diversity enables better adaptation to changes.

Table 2.3 presents the general differences between TAD and MAD in some key performance parameters of anaerobic digestion, which may differ based on other used process parameters.

Table 2.3 General differences between TAD and MAD, which may differ based on other process parameters used (adapted from De la Rubia et al., 2013; Schnürer & Jarvis, 2018*).*

Parameter	**TAD**	**MAD**
Substrate degradation rate	Higher	Lower
Biogas production	Higher	Lower
Volatile solids reduction	Higher	Lower
Pathogen reduction	Higher	Lower
Reactor volume	Lower	Higher
Alkalinity	Higher	Lower
Heat and energy recovery	Higher	Lower
VFA accumulation	Higher	Lower
Ammonia concentration	Higher	Lower
Energy input	Higher	Lower
Risk for process instability	Higher	Lower
Microbial diversity	Lower	Higher
Resistance to foaming	Higher	Lower

Kardos et al. (2011) conducted a comparative study of MAD and TAD of sewage sludge in full-scale anaerobic reactors at a municipal wastewater treatment plant (WWTP). The findings revealed that TAD exhibited a higher average specific biogas output compared to MAD. Moreover, the methane content of biogas was higher in TAD (59%) than in MAD (54%). Although alkalinity was higher in the mesophilic system, both systems demonstrated sufficient buffer capacity for process stability. The thermophilic system showed increased volatile acid concentration and utilization, as confirmed by larger specific gas production data.

In another study, Ferrer et al. (2011) compared MAD and TAD from an energy perspective across lab-scale, pilot-scale, and full-scale anaerobic reactors operating

under various conditions. The results indicated that thermophilic digesters with half the solid retention time (SRT) of mesophilic digesters exhibited comparable performance. This suggested that converting MAD to TAD could potentially reduce digester volume or increase system loading rates, leading to operational cost savings. Additionally, the study found that anaerobic digesters could be net energy producers, with the most favourable outcomes achieved at low SRT (10–15 days) and high organic loading rates (OLR) (2–3 kg VS/m^3/d), which is possible in TAD.

Furthermore, Lanko (2021) compared mesophilic (38 °C), thermophilic (57 °C), and temperature-phased AD of sewage sludge in a lab-scale study using WAS as substrate and employing simple mixing mechanisms. The results showed that TAD had better organic matter removal and methane production compared to MAD. TAD also showed better pathogen deactivation in the digestate, potentially allowing for its direct application in agriculture. Additionally, a life cycle assessment of the three systems revealed TAD to be the most environmentally friendly option for sewage sludge treatment.

2.5 Influence of biochar on anaerobic digestion

Biochar is a carbon-rich porous material produced by the pyrolysis of biomass with limited or no oxygen. Its physical and chemical composition varies depending on production methods, influenced by factors like original feedstock and pyrolysis conditions such as temperature, heat transfer rate, and residence time (Fransson et al., 2020). As a result, biochar can closely resemble the original material or transform into graphite-like charcoal with carbon atoms arranged in hexagonal rings, bound to various functional groups present in the feedstock. Pyrolysis-induced physiochemical changes give biochar many of its properties like large specific surface area, high porosity, presence of functional groups, pH buffering capacity, strong adsorption, and good electrical conductivity (Tan et al., 2014).

The production of biochar from dried sewage sludge is gaining traction as a sustainable method for sludge management at WWTPs. Thermochemical conversion of sewage sludge into sludge biochar reduces sludge volume, minimizing its disposal costs. Moreover, the high pyrolysis temperature can also eliminate pathogens in the sludge, producing environmentally safe biochar with versatile applications. In Sweden, there are ongoing projects which aim to conduct pilot-scale studies on sewage sludge pyrolysis and explore potential beneficial applications of the produced sludge biochar (Sweden Water Research, 2024).

The use of biochar as an additive in anaerobic digestion has been studied extensively in recent times. Studies suggest that biochar additives can enhance and stabilize biochemical reactions during anaerobic digestion, facilitating faster process start-up, increased methane yield, and process stability (Tang et al., 2020). Table 2.4 presents results from some of these studies, demonstrating biochar's potential to improve anaerobic digester performance.

Table 2.4 Results from previous studies showing enhancement of anaerobic digestion performance using biochar as additives.

BC feedstock	BC characteristics and dose	AD feedstock	AD process parameters	Observed AD performance	Reference
Sewage sludge	BC1 pyrolysis at 350 °C, pH 6.4 BC2 pyrolysis at 550 °C, pH 9.5 Dose 1.25, 2.5, 3.75, 5 g/l	Fruit wastes	Batch test, 400 ml Mesophilic (37 °C)	Methane yield increased by 16 to 33% with optimum dose at 2.5 g/l for BC1 and 3.75 g/l for BC2	(Ambaye et al., 2020)
Sewage sludge	600 C pH 9.7 Dose 6.2, 15.9, 26.1, 34.2 g/l	Municipal WWTP sludge	Batch test, 500 ml Mesophilic (35 °C)	Methane production increased by 10%, 22% and 33% in first three dosages whereas it decreased by 2% with a high dose of 34.2 g/l	(Zhang et al., 2019)
Sewage sludge	BC1 pyrolysis at 300 °C, pH 6.78 BC2 pyrolysis at 500 °C, pH 7.5 BC3 pyrolysis at 700 °C, pH 7.92 Dose 10g/l	WAS from municipal WWTP	Batch test, 500 ml Mesophilic (37 °C)	Methane production increased by 19%, 10% and 3% with BC1, BC2 and BC3 respectively	(Wu et al., 2019)
Sawdust	500 °C Dose: 10 g/l	WAS + food waste	Batch test, 120 ml Thermophilic (55 °C)	Lag phase decreased to 2 days compared to up to 18 days without biochar	(Li et al., 2018)
Forestry waste	450–550 °C, pH 8.1 Dose 8.5 g/g VS inoculum	Acidified mixed sludge from WWTP	Lab-scale, 160 ml Thermophilic (55 °C)	Lag phase decreased to 4 days from 12 to 52 days without biochar	(Khoei et al., 2021)

2.5.1 Biochar mechanisms in enhancement of anaerobic digestion

The stability and efficiency of the AD process depends on the balance among its four stages of biochemical reactions. Disruption can occur due to slow degradation of feedstocks, accumulation of intermediate products, and inhibition of methanogen activities (Schnürer & Jarvis, 2018). With properties like having a large specific surface area and good buffering and adsorption capacities, biochar use could result in reducing process imbalances, thereby enhancing digestion performance. Studies by Pan et al. (2019) and Qiu et al. (2019) show how these positive effects could be the result of specific biochar mechanisms. The following sections describe these biochar mechanisms and their potential to improve digestion performance.

2.5.1.1 Effect on pH and VFA accumulation

AD processes exhibit optimal performance within neutral to slightly alkaline pH range (between 7.0 and 8.5), and there is a potential decrease in the activity of the methanogens when the pH falls outside this range (Schnürer & Jarvis, 2018). Maintaining this optimal pH during the digestion process depends on the balance between the production and degradation of VFAs, the main intermediate products in AD. Rapid VFA accumulation, particularly at high organic loading rates and with easily acidifiable substrates, can result in pH reduction, inhibiting the metabolic activities of methanogens.

Biochar, with its alkaline functional groups, possesses a good buffering capacity that can effectively neutralize the generated VFAs and prevent rapid pH drops. Shen et al. (2015) tested the effects of corn stover biochar on thermophilic anaerobic digestion of sewage sludge and found that the alkaline functional groups existing on the surface of biochar helped maintain the optimal pH of 7.5 to 8, increasing process stability. Another study by Wang et al. (2018) investigated the effects of 12 types of biochar derived from various biomass sources (sawdust, wheat bran, peanut shell and sewage sludge) in mesophilic co-digestion of food waste and sewage sludge and discovered that biochar promoted the production of the easily utilized acetate over other difficult to degrade VFAs. Additionally, biochar's excellent adsorptive capacity allows it to adsorb accumulated VFAs, preventing process slowdown due to acid accumulation.

2.5.1.2 Effect on overcoming ammonia inhibition

Ammonia is produced during the biological degradation of nitrogen-rich substrates like food waste, manure, or sewage sludge. While it serves as a crucial nitrogen source for anaerobic microorganisms, high concentrations of ammonia can inhibit methane production during anaerobic digestion (Schnürer & Jarvis, 2018). High concentrations of total ammonia nitrogen (TAN) have been observed to cause inhibition of specific biochemical reactions leading to a disruption in the digestion process (Sharma & Melkania, 2017). In digesters, ammonia exists primarily as free ammonia (NH_3) and ammonium ion (NH_4^+), with free ammonia exerting a stronger inhibitory effect by adversely affecting microorganisms at the cellular level.

Biochar use has been found to reduce TAN through physical and chemical adsorption mechanisms. The adsorption capacity of biochar depends on its physiochemical properties, influenced by the original material and pyrolysis process. Studies have shown that adsorptive capacity increases with specific surface area and the presence of certain functional groups (Wang et al., 2018; Koukouzas et al., 2007). Biochar containing acidic groups, sulphur groups, alkali earth metals, and other metals may facilitate chemical catalytic reactions that enhance the adsorption of ammonia and other compounds. There is also the possibility that the microorganisms growing on biochar surfaces and forming biofilms could be more resilient and effective in overcoming ammonia inhibition compared to suspended microorganisms (Sossa et al., 2004).

2.5.1.3 Role in interspecies electron transfer

Among the two main methanogenesis pathways, hydrogenotrophic methanogenesis relies on the symbiotic relationship between SAOB and hydrogen consuming methanogens to overcome thermodynamic barriers. In this process, hydrogen can be

considered a diffusive electron carrier, and this process is thermodynamically feasible only if the hydrogen produced by the SAOB is efficiently utilised by the hydrogen-consuming methanogens (Uddin & Wright, 2021). Interspecies electron transfer (IET) facilitates this mutualistic symbiosis, wherein electron donor microorganisms transfer electrons to electron acceptor microorganisms through either direct cell contact (direct IET) or indirect pathways mediated by intermediates (indirect IET), enabling metabolic processes that are difficult for a single microorganism to accomplish (Su et al., 2023).

The use of biochar in the AD process has been found to promote direct interspecies electron transfer (DIET) (Baek et al., 2018). Unlike indirect pathways reliant on intermediates like hydrogen, DIET occurs directly on the surface of biochar, facilitating electron exchange between SAOB and methanogen communities. Biochar can support the growth of DIET-capable microorganisms, effectively serving as electrical conduits for electron exchange. This mechanism enables much faster electron transfer velocities between microorganisms resulting in faster degradation of the substrate and intermediates.

2.5.1.4 Role in enrichment of functional microbes

Biochar possesses properties such as a large specific surface area and porous structure, making it an effective carrier material that promotes the formation of biofilms and enhances microbial abundance in AD. In addition to promoting growth of DIET capable microorganisms, biochar can also promote the growth of other selective microbial groups. Different types of biochar have been shown to enrich the abundance of specific microbial species that can improve digestion performance (Dang et al., 2016). Huggins et al., (2016) noted that biochar pore sizes ranged from 1 to 40 μm, providing ample space to accommodate microorganisms. Additionally, Zhang et al., (2017) observed that biochar stimulated the secretion of extracellular polymeric substances, enhancing microorganism adhesion to the carrier surface during biofilm formation.

2.6 Experimental determination of biogas yield through batch tests

Experimental assessment of biogas yield from anaerobic digestion of various test substrates can be conducted through laboratory-scale experiments using either discontinuous (batch) or continuous stirred tank reactor (CSTR) methods (Weinrich et al., 2018). Continuous experiments give a better representation of the conditions of continuously operated anaerobic digestion plants, but they are more laborious and time consuming to perform at the lab scale. In contrast, batch tests are simpler to conduct and can offer valuable preliminary insights into the anaerobic biodegradability of test substrates.

In batch tests, a known quantity of the test substrate is placed in a closed, airtight glass vessel under mesophilic or thermophilic temperature conditions, and gas production is monitored over time. The glass vessel contains an empty headspace for gas formation, and the internal pressure is vented after each measurement. Gas measurement can be performed using volumetric, manometric, or pressure transducer methods.

The simpler batch method for estimating the biochemical methane potential (BMP) of feed sources in anaerobic treatment was first developed by Owen et al. (1979) and has since been widely used in biogas potential studies, with or without modifications.

Efforts to standardize the test protocol for improved accuracy and reliability of results have led to guidelines provided by Angelidaki et al. (2009), Holliger et al. (2016), and VDI 4630 (2016). These guidelines cover parameters such as substrate selection, inoculum source, experimental setup, monitoring parameters, test duration, replication and controls, and data analysis.

2.6.1 Theoretical biogas potential

The theoretical biogas potential of a specific substrate serves as a benchmark, indicating the maximum biogas yield achievable through AD and providing valuable insight into digestion performance. If the chemical composition of the organic substrate is known, its theoretical biogas potential can be stoichiometrically calculated using the model proposed by Buswell & Mueller (1952), as represented by Equation 2.14. This model assumes complete stoichiometric conversion of the organic substrate into methane and carbon dioxide.

For more complex substrates containing nitrogen and sulfur, Buswell's model was modified by Boyle (1977) to incorporate the production of ammonia and hydrogen sulfide during digestion (Equation 2.15). However, it is important to note that the actual biogas potential of any substrate is always lower than the theoretical potential. This discrepancy arises because the microorganisms involved in anaerobic digestion utilize some portion of the substrate for their own growth and maintenance, thereby reducing the amount of degradable substrate available for biogas production.

$$C_aH_bO_c + \left(a - \frac{b}{4} - \frac{c}{2}\right) H_2O \rightarrow \left(\frac{a}{2} - \frac{b}{8} + \frac{c}{4}\right) CO_2 + \left(\frac{a}{2} + \frac{b}{8} - \frac{c}{4}\right) CH_4$$

[Equation 2.14]

$$C_aH_bO_cN_dS_e + \left(a - \frac{b}{4} - \frac{c}{2} + \frac{3d}{4} + \frac{e}{2}\right) H_2O$$
$$\rightarrow \left(\frac{a}{2} - \frac{b}{8} + \frac{c}{4} + \frac{3d}{8} + \frac{e}{4}\right) CO_2 + \left(\frac{a}{2} + \frac{b}{8} - \frac{c}{4} - \frac{3d}{8} + \frac{e}{4}\right) CH_4 + dNH_3 + eH_2S$$

[Equation 2.15]

In experiments, especially those employing simple substrates like glucose or cellulose as controls, comparing the actual biogas yield with the theoretical yield is pivotal for validating experimental results. Weissbach (2009) has presented theoretical and effective biogas potential data for various groups of organic substrates, some of which are summarised in Table 2.5.

Table 2.5 Methane percentage, theoretical methane yield and theoretical biogas yield of some organic compounds (adapted from Weissbach, 2009*).*

Substrate	Chemical composition	Methane %	Theoretical methane yield (ml/g VS)	Theoretical biogas yield (ml/g VS)
Carbohydrate (Glucose)	$C_6H_{12}O_6$	50	373	746
Carbohydrate (Cellulose)	$C_5H_{10}O_5$	50	415	829
Alcohol (Methanol)	CH_4O	75	525	699
Alcohol (Ethanol)	C_2H_6O	75	730	973
Protein (Alanin)	$C_3H_7O_2N$	50	473	946
Protein (Lycin)	$C_6H_{14}O_2N_2$	58.3	612	1049
Lipid (Palmitic acid triglyceride)	$C_{51}H_{98}O_6$	71.1	1006	1416
Lipid (Stearic acid triglyceride)	$C_{57}H_{110}O_6$	71.5	1024	1433

3 Methods

This section outlines the methodology adopted for carrying out this thesis project.

3.1 Literature review

A literature review was first conducted using the scientific databases Google Scholar and Scopus. The literature review focused on the following thematic areas:

- Anaerobic digestion process mechanism
- Effect of temperature on anaerobic digestion at WWTPs
- Effect of using biochar as an additive in anaerobic digestion
- Standard protocols for conducting anaerobic digestion batch experiments

3.2 Experimental work

3.2.1 Design of batch test

The experiment was carried out using 300 ml glass bottles as batch anaerobic reactors. A total of 13 bottles were used, categorised into four triplicate groups: Group A (A1, A2, A3), Group B (B1, B2, B3), Group C (C1, C2, C3), and Group D (D1, D2, D3), alongside a single blank reactor E, as illustrated in Figure 3.1.

Groups A, B, C, and the blank reactor E were consistently maintained at 55 °C inside an incubator throughout the experimental period to sustain thermophilic conditions (Setup 1), while Group D was kept at room temperature (Setup 2).

The experiment was carried out in two consecutive phases, with each phase examining the impact of additives on anaerobic digestion using distinct substrates. Phase 1 utilized microcrystalline cellulose ($(C_6H_{10}O_5)_n$ as the substrate, while Phase 2 employed anhydrous sodium acetate (CH_3COONa). Both these substrates had known chemical compositions allowing for the calculation of their theoretical biogas potential.

Throughout both phases, reactor groups A, B, C, and D received inoculum and substrate, while the blank reactor E only received inoculum to measure the background biogas production. Furthermore, Group A reactors were supplemented with synthetic graphite (SG), and Group B reactors with sludge biochar (SB) as additives. Group C served as the control, receiving only inoculum and substrate without additives, whereas Group D received the same without additives but was maintained at room temperature.

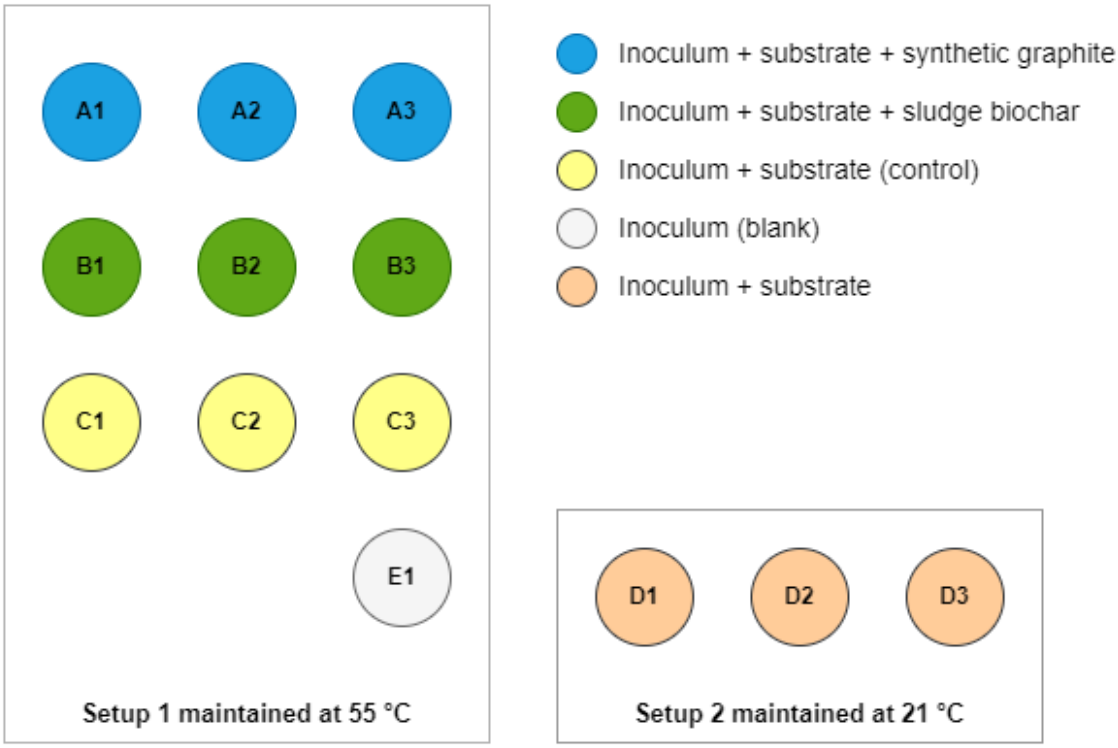

Figure 3.1 Schematic arrangement of experimental setup.

3.2.2 Inoculum, substrate and additive characteristics

The inoculum used in the experiment was collected from one of the three mesophilic digesters at Ryaverket WWTP in Gothenburg on 20 February 2024. These digesters operated at a temperature of 35–36 °C, with a retention period of 18–20 days and an organic loading rate of 2.6 kg VS/m^3-d. The digesters were fed continuously with mixed sludge consisting of PS and WAS in equal proportions. Based on data from the previous year, the average total solids (TS) and volatile solids (VS) content of the digested sludge was 3.5 % and 2.12 % respectively (D. Lorick, personal communication, Feb. 28, 2024).

The experiment used two different substrates in each phase to investigate the impact of additives on their anaerobic digestion. In the first phase, microcrystalline cellulose (CAS Number: 9004-34-6, Sigma-Aldrich, powder, 20 µm) was used as the substrate, which is a widely used control substrate in anaerobic digestion batch tests (Figure 3.2). This substrate offers several advantages, including a precisely defined chemical composition that facilitates straightforward calculation of its theoretical biogas potential. Moreover, being a natural carbohydrate, it undergoes all four stages of anaerobic digestion.

In the second phase, anhydrous sodium acetate (CAS Number: 127-09-3, Sigma-Aldrich, purity ≥ 99%) was used as the substrate (Figure 3.2). Unlike microcrystalline cellulose, sodium acetate is an organic salt that readily dissolves in water to produce acetate ions, the primary substrate for methane production. This characteristic allows for the occurrence of only the final stage of anaerobic digestion, specifically targeting the methanogenesis reactions to assess the impact of additives.

The experiment utilized two different additives to assess their impact on anaerobic digestion performance. The primary focus of this study was sludge biochar, which was

added to reactors B1, B2, and B3. This biochar was produced from pyrolysis of dried sewage sludge at 650°C and was supplied by Va Syd AB (Figure 3.3). It originated from dewatered sewage sludge at Fårevejle WWTP in Denmark and underwent integrated steam drying and pyrolysis at the AquaGreen pyrolysis plant in Fårevejle on December 20, 2023, as part of the Testbed Ellinge Project.

Synthetic graphite (ProGraphite GmbH, coarse granular, 0.7–2 mm, carbon purity ≥ 99%) was used as the second additive and was added in reactors A1, A2 and A3 (Figure 3.3). Synthetic graphite is manufactured by high temperature processing of amorphous carbon materials derived from petroleum, coal, etc. It was selected as a second additive for comparison with sludge biochar, as previous studies have indicated its positive effects on anaerobic digestion performance (Xie et al., 2020).

Figure 3.2 Substrates used in the experiment: microcrystalline cellulose (left) and anhydrous sodium acetate (right).

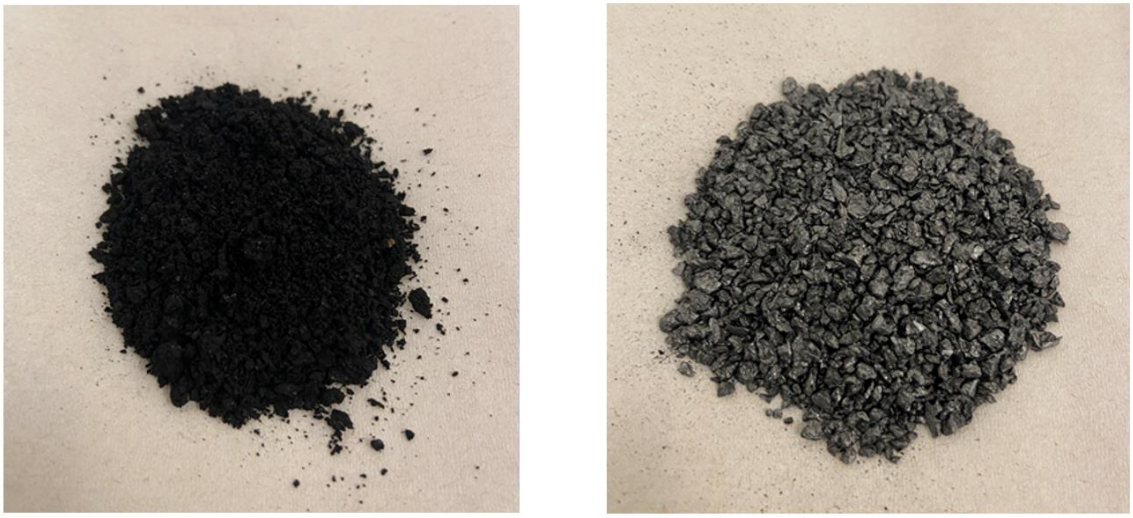

Figure 3.3 Additives used in the experiment: sludge biochar (left) and synthetic graphite (right).

3.2.3 Total solids and volatile solids analysis

Total solids content (TS) refers to the materials that remain as residue after the sample has been dried at 105 °C for 24 hours, whereas volatile solids content (VS) represent the measure of organic content present in the sample and refers to the amount of total solids lost when the sample is combusted at 550 °C in the presence of excess air. Both TS and VS content of the inoculum was calculated prior to the start of the experiment using the standard method outlined in APHA (2017). It was also calculated for the reactor samples in all 13 test reactors after the end of the experiment. The following steps were followed for their calculation:

i. The empty dish was weighed, and its value recorded as W1.
ii. A known volume of sample (30 ml for inoculum, 25 ml for reactor samples) was added in the dish and the weight of dish with sample was recorded as W2.
iii. The dish with sample was placed in an oven at 105 °C for 24 hours.
iv. After 24 hours, the dish was taken out, cooled, and weighed again with remaining solid contents to give W3.
v. After recording W3, the dish was put inside a pre-heated furnace at 550 °C for 20–30 minutes.
vi. The dish was taken out, allowed to cool and then weighed again to give W4.

After this, TS and VS were calculated using Equations 3.1 – 3.4.

$$TS\ (mg/l) = \frac{(W3 - W1) * 1000}{sample\ volume\ in\ ml} \quad \text{[Equation 3.1]}$$

$$VS\ (mg/l) = \frac{(W3 - W4) * 1000}{sample\ volume\ in\ ml} \quad \text{[Equation 3.2]}$$

$$TS\ \%\ (w/w) = \frac{TS\ in\ mg/l}{10000} \quad \text{[Equation 3.3]}$$

$$VS\ \%\ (w/w) = \frac{VS\ in\ mg/l}{10000} \quad \text{[Equation 3.4]}$$

3.2.4 Alkalinity test

Alkalinity of the sludge biochar, synthetic graphite and inoculum samples was determined by potentiometric titration method reducing the pH of sample to 4.5 based on APHA (2017) method. Hydrochloric acid (0.05 M) was used as the standard acid which was gradually added to the test samples until the pH was reduced to 4.5. The test was carried out with following steps.

1. 3 test samples were prepared consisting of
    i. 5 g of SG in 100 ml of water
    ii. 5 g of SB in 100 ml of water
    iii. 50 ml of inoculum diluted to 250 ml sample
2. The initial pH for each of the samples was measured using a pH meter and recorded.
3. The samples were stirred uniformly using magnetic stirrers while known volume of standard acid was added until the pH dropped to 4.5.
4. The volume of acid added in each step and the corresponding change in pH was recorded until the pH reached 4.5.

After this, alkalinity of the samples was calculated using Equation 3.5.

$$Alkalinity\ (mg\ CaCO3/L) = \frac{A*N*50000}{sample\ volume\ in\ mL} \quad \text{[Equation 3.5]}$$

where A = total volume of standard acid used (ml)

N = normality of standard acid

The calculated alkalinity values were then normalized to the mass of added SG and SB and the volume of undiluted inoculum to determine the contribution of alkalinity from the additives and inoculum in the test reactors.

3.2.5 Electrical conductivity and pH of reactor samples

After the end of experiment, the electrical conductivity and pH of the reactor samples from all 13 test reactors was measured using EC meter and pH meter. Electrical conductivity values were indicative of the salinity levels in the reactors at the end of digestion.

3.2.6 Performance of batch test

3.2.6.1 Preparation of reactors for Phase 1

The glass bottles used in the experiment had a total available volume of 323.21 ml which was calculated by weighing the bottles when empty and when filled with water. To have a good working volume and sufficient reactor headspace for biogas production, all 13 reactors were fed to a working volume of 150 ml leaving a head space volume of 173.21 ml. The working volume constituted of inoculum, substrate and additives.

Based on the recommendation from Holliger et al. (2016), an inoculum to substrate ratio (ISR) of 2:1 was adopted for Phase 1 of the experiment. This was done to have the portion of VS from the inoculum greater than that from the substrate to minimize acidification or inhibition problems during the batch test. A VS content of 2% was assumed for the inoculum at the start of the experiment based on previous year averages for Ryaverket WWTP. Based on this, all 13 reactors were filled with 150 ml of inoculum to give an inoculum concentration of 3 g VS per reactor.

For the substrate, a VS content ≥ 99% was assumed which resulted in the addition of 1.5 g microcrystalline cellulose per reactor to maintain the adopted ISR of 2:1. Based on its chemical composition, 1.5 g of microcrystalline cellulose amounted to 0.67 g of carbon per reactor. Figures 3.4 – 3.6 show the preparation of reactors at the start of Phase 1.

For the addition of additives, a higher concentration of 50 g/l was adopted resulting in the addition of 7.5 g of synthetic graphite in Group A reactors and 7.5 g of sludge biochar in Group B reactors. Due to the short time frame of this study, only a single concentration of the additive was tested. However, Zhang et al., (2019) has observed that the effect of additives can vary based on different doses which can be the scope of future investigations. Appendix A shows the calculations for the initial dose of inoculum, substrate and additives before the start of the experiment.

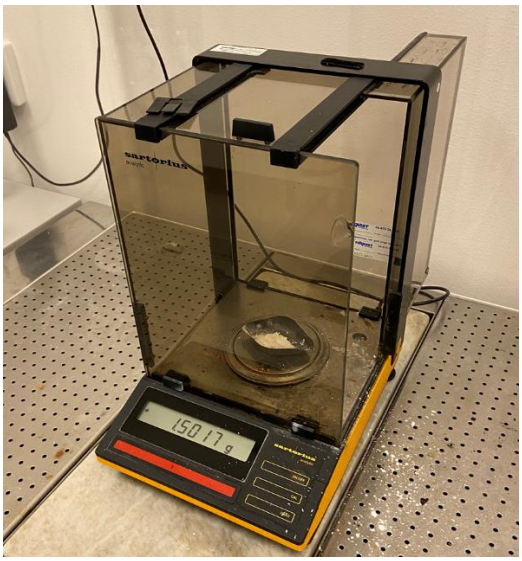

Figure 3.4 Weighing 1.5 g of substrate for the first phase of the experiment.

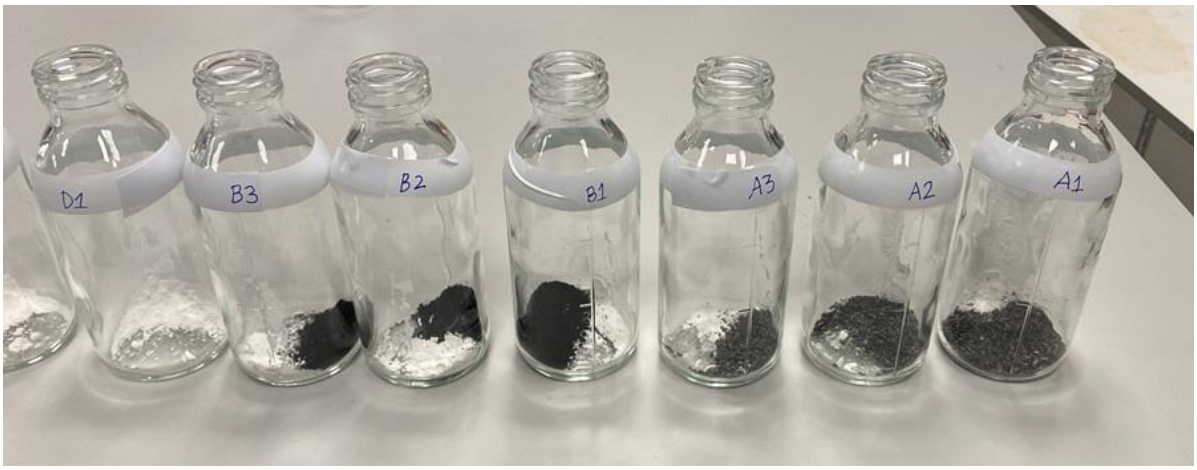

Figure 3.5 Test reactors after receiving 1.5 g substrate and 7.5 g additive at the start of first phase of the experiment.

Figure 3.6 Sealed test reactors after the addition of inoculum, substrate and additives at the start of first phase of the experiment.

3.2.6.2 Start and maintenance of batch test

Following the addition of inoculum, substrate and additives, the reactors were flushed with nitrogen gas for about 30 seconds before being closed with butyl rubber septa and aluminium crimp cap to maintain anaerobic conditions. Reactors from Group A, B, C and the blank E were kept inside an incubator at 55 °C (Figure 3.7) while Group D reactors were maintained at room temperature of 21 °C inside a fume hood.

Daily measurements of headspace pressure, resulting from biogas production, was taken for all 13 reactors by inserting a syringe needle through the butyl rubber septa. This needle was connected to a pressure transducer (Model AP-13S, Keyence Corporation, Japan), which quantified the pressure inside the reactor in kilopascals (kPa) relative to atmospheric pressure. Figures 3.8 and 3.9 illustrate a schematic representation of the reactor setup and the measurement process.

Before each measurement, the reactors were gently swirled to allow for proper mixing of the contents. After recording the measured pressure value, the produced biogas was vented out through the needle until the headspace pressure returned to zero (Figure 3.10). These daily pressure measurements were conducted as swiftly as possible to minimize temperature fluctuations, particularly for the thermophilic reactors when removed from the incubator. When it was not possible to access the lab during weekends and on public holidays, the reading measured on the first day after the gap was averaged over the missed days to have a continuous series of measured data. For example, if there was a reading on Day 15 (Friday) and then the next reading was on Day 18 (Monday), the reading on Day 18 was divided by 3 and averaged over Day 16, 17 and 18. The daily measurement routine was continued until the daily biogas production in the reactors fell below 1% of the cumulative biogas yield.

Figure 3.7 Maintenance of test reactors inside an incubator at 55 °C.

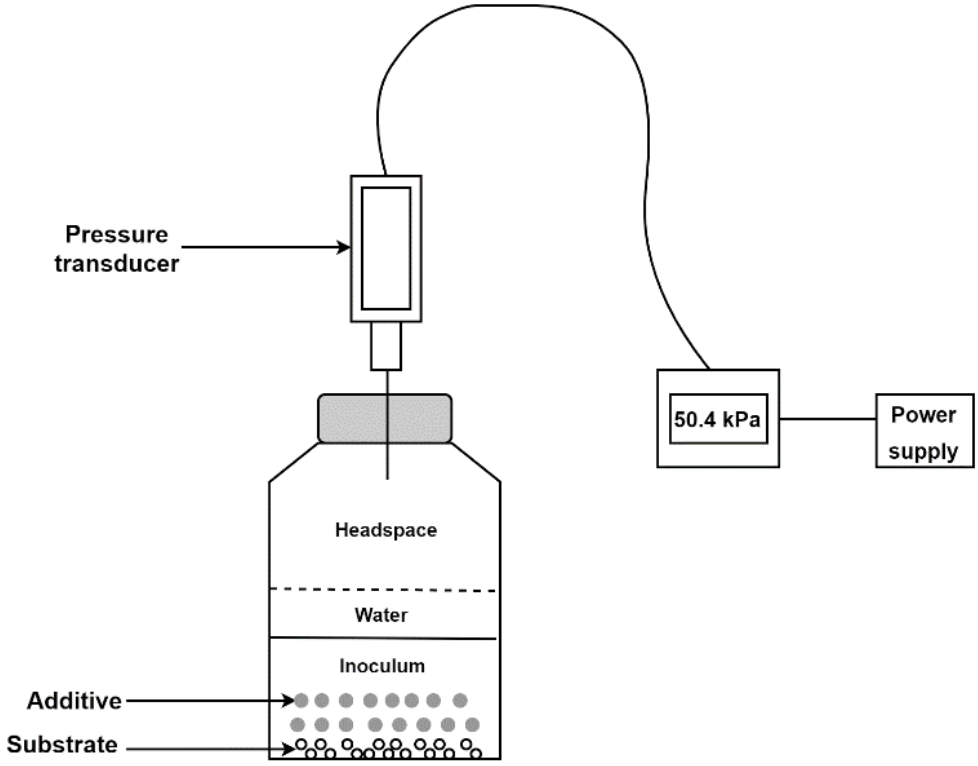

Figure 3.8 Schematic illustration showing process of headspace pressure measurement in the test reactors.

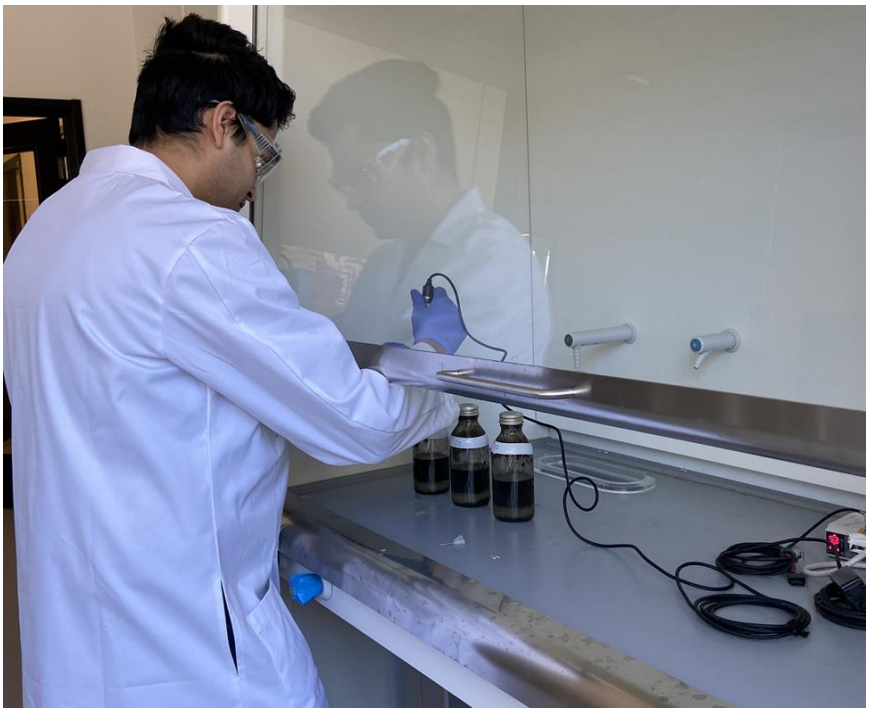

Figure 3.9 Daily pressure measurement in the reactors using pressure transducer.

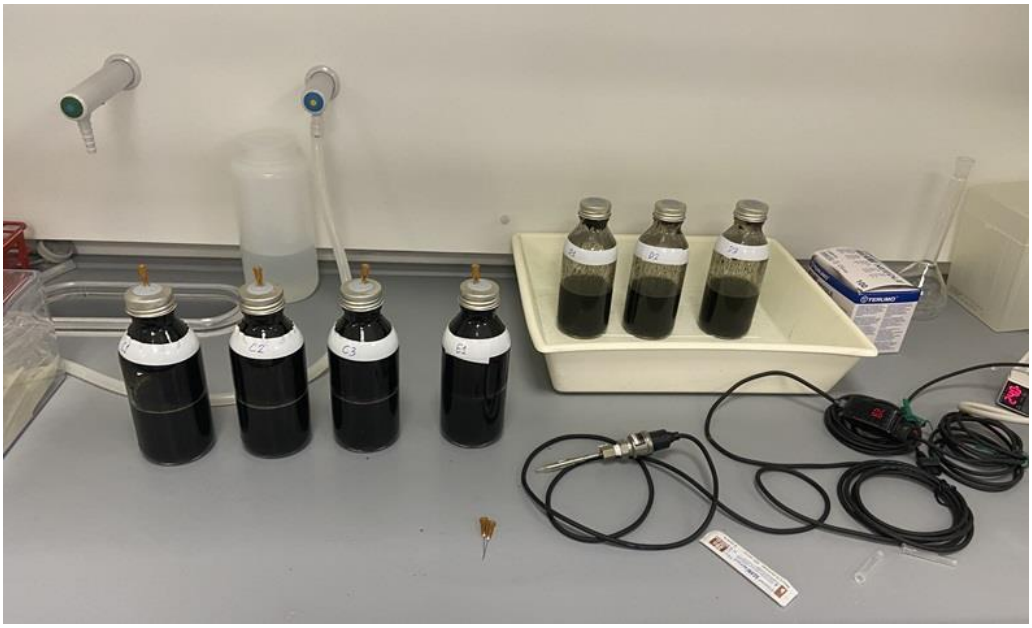

Figure 3.10 Releasing the produced biogas through the inserted needles after each measurement.

3.2.6.3 Preparation of reactors for Phase 2

Once the daily biogas production in the reactors fell below 1% of the cumulative biogas yield, it indicated the completion of anaerobic digestion in Phase 1. After this, the reactors were opened and about 5 ml of reactor sample was collected from all 13 reactors for analysis. The working volume in the reactors was restored back to 150 ml by adding 5 ml of water.

After this, 2.28 g of anhydrous sodium acetate (CH_3COONa) was added as the second substrate to Group A, B, C and D reactors, maintaining a carbon content of 0.67 g per reactor, similar to that from microcrystalline cellulose in Phase 1 (Figure 3.11). The additives added to Group A and B reactors during Phase 1 remained unchanged for Phase 2.

Following this, the reactors were again flushed with nitrogen gas for about 30 seconds before being resealed with butyl rubber septa and aluminium crimp cap to maintain anaerobic conditions. After this, the daily pressure readings in the reactors was continued similar to that in Phase 1, until the daily biogas production fell below 1% of the cumulative biogas yield.

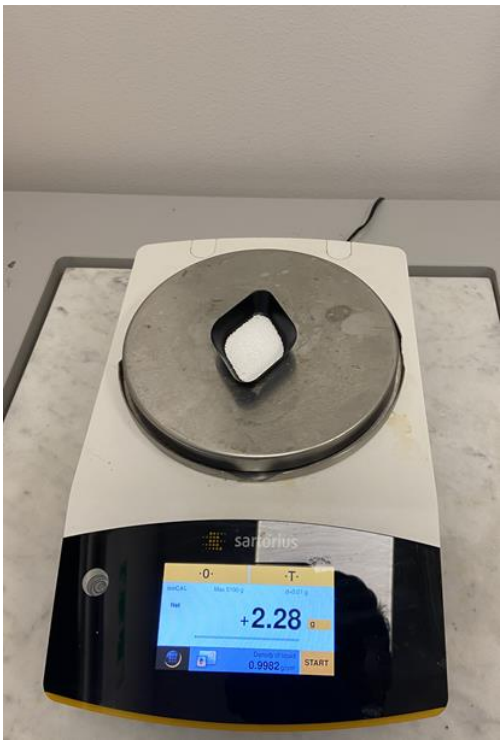

Figure 3.11 Weighing 2.28 g of sodium acetate at the start of second phase of the experiment.

3.2.7 Calculation of biogas data

3.2.7.1 Biogas volume calculation

Using the ideal gas equation (Equation 3.6), the measured headspace pressure inside each reactor was converted into the number of moles of produced biogas. This general equation offers a reliable approximation of gas behaviour under varied conditions. Throughout the experiment, the reactor headspace volume (V) and temperature (T) remained constant parameters, while the headspace pressure (P) and number of gas moles inside the reactor (n) changed with biogas production. It was assumed that the produced biogas consisted of only methane and carbon dioxide since the used substrates were simple and did not contain nitrogen and sulphur which can lead to production of other gases like nitrogen, ammonia and hydrogen sulphide.

The effect of vapour pressure and the high water solubility of carbon dioxide was not considered while calculating the biogas volume. After computing the number of moles of produced biogas at reactor temperature using Equation 3.1, the same equation was utilized to convert the calculated moles into biogas volume at standard temperature and pressure (STP) conditions. For this conversion, the adopted STP values were 273.15 Kelvin temperature and 101.325 kPa pressure. This standardization facilitated the comparison of produced biogas volumes across different reactors at STP conditions. Sample calculations demonstrating the determination of the number of moles of produced biogas and its subsequent conversion to biogas volume at STP conditions is shown in Appendix B.

$$PV = nRT \qquad \text{[Equation 3.6]}$$

where P = headspace pressure due to produced biogas

V = reactor headspace volume (0.000173 m^3)

n = number of moles of biogas produced

R = universal gas constant (8.314 Pa m^3/mol K)

T = temperature in Kelvin (328.15 K for Setup 1 and 294.15 K for Setup 2)

3.2.7.2 Theoretical biogas potential

Previous studies by Wang et al., (2014) and Weinrich et al. (2018) calculated the theoretical biogas potential of cellulose to be 829 ml/g VS at STP conditions, based on the model of Buswell & Mueller (1952). Using this value, the theoretical biogas yield for 1.5 g of microcrystalline cellulose was calculated to be 1245 ml at STP conditions. The calculation for this has been shown in Appendix C.

For estimating the theoretical biogas potential of sodium acetate, a manual stoichiometric approach was adopted since sodium acetate did not undergo all four stages of anaerobic digestion and only underwent the methanogenesis stage. Stoichiometric calculation was carried out for the two-step methanogenesis reaction (Equation 2.2a and 2.2b), consisting of the syntrophic acetate oxidation and subsequent hydrogenotrophic methanogenesis, as it has been found to be the dominant methanogenesis pathway in thermophilic conditions (Dyksma et al., 2020). Assuming a methane to carbon dioxide ratio of 50:50, the theoretical biogas potential of 2.28 g of sodium acetate was calculated to be 1246 ml at STP conditions. The calculation for this has been shown in Appendix C.

3.2.8 Statistical analysis

The biogas volume produced in each triplicate group was recorded as the mean value with standard deviation (Mean ± SD). To assess potential statistical differences among the mean production in Groups A, B, and C, a single-factor ANOVA ($p \leq 0.05$) was conducted on the biogas yields using MS Excel. Furthermore, a two-tailed Student's t-test, accounting for unequal variance and a 95% confidence interval, compared the results between Groups A and B with those of Group C. Dixon's test was employed to identify any significant outliers within the triplicate readings. Additionally, the

coefficient of variation was computed for each group, with a CV less than 10% deemed indicative of reliable measurements.

4 Results and discussion

The findings from the experiment are discussed in this section.

4.1 TS and VS analysis

The results from TS and VS analysis of the inoculum are presented in Table 4.1. Given the high purity of both substrates, it was assumed that they had a VS content ≥ 99%. Results show that the actual VS for the inoculum sample was less than the assumed 2%, which was used to calculate the mass of substrate added in each reactor at the start of the experiment. This indicates that the actual ISR in the reactors was 1.64, meaning that the substrate availability to the microorganisms was higher than it would have been at a VS of 2%.

Table 4.1 Results from TS and VS analysis of inoculum before the start of experiment.

Sample	**TS% (w/w)**	**VS% (w/w)**	**VS/TS (%)**	**Remarks**
Inoculum	2.63 ± 0.07	1.64 ± 0.04	62.5	From test
Microcrystalline cellulose	≥ 99	≥ 99	100	Assumed
Sodium acetate	≥ 99	≥ 99	100	Assumed

Following the completion of Phase 2, the TS and VS content of all 13 reactor samples was measured, which is presented in Table 4.2. Notably, the TS and VS content in the thermophilic reactors was lower than that of Group D reactors maintained at room temperature. This difference could be attributed to the higher substrate degradation rate observed at 55 °C compared to 21 °C, resulting in reduced TS and VS content. Within the thermophilic reactors, the VS content remained consistent at around 1.45% across all three groups, while the TS content varied from 3.29% in Group C to 3.53% in Group B. The TS and VS content in the blank reactor was the lowest at 2.32% and 1.20% respectively.

Table 4.2 Results from TS and VS analysis of reactor samples after the end of Phase 2 of the experiment.

Reactor	**TS% (w/w)**	**VS% (w/w)**	**VS/TS (%)**
Group A (A1, A2, A3)	3.40 ± 0.07	1.45 ± 0.07	42.7
Group B (B1, B2, B3)	3.53 ± 0.20	1.45 ± 0.10	41.1
Group C (C1, C2, C3)	3.29 ± 0.07	1.44 ± 0.03	43.7
Group D (D1, D2, D3)	4.08 ± 0.03	2.07 ± 0.02	50.6
Blank (E)	2.32	1.20	51.7

4.2 Alkalinity test

The measured total alkalinity values for synthetic graphite, sludge biochar, and inoculum samples are presented in Table 4.3, while Table 4.4 presents their normalized alkalinity values. Figure 4.1 illustrates the pH decrease across the three samples after acid addition during titration, confirming the higher buffering capacity of SB compared to SG.

Initially, the pH of the synthetic graphite sample was acidic, measuring 6.1, whereas that of the sludge biochar and inoculum samples was alkaline, at 7.8 and 7.4 respectively. The calculated alkalinity for the inoculum was 5219 mg $CaCO_3$/l which met the alkalinity quality criteria as recommended by Holliger et al. (2016).

Comparing the two additives, the alkalinity of sludge biochar measured notably higher at 40 mg $CaCO_3$/l which was 16 times more than that for synthetic graphite, measured at 2.5 mg $CaCO_3$/l. The higher alkalinity of sludge biochar means it has a greater buffering capacity to acid accumulation which is a common problem during anaerobic digestion. This higher buffering capacity of sludge biochar could be beneficial in resisting the pH fluctuation caused by the production and accumulation of intermediate products during substrate degradation.

However, looking at the normalised alkalinity values (Table 4.4), it is clear that over 99% of the alkalinity in the test reactors originated from the inoculum, suggesting minimal impact from the additives on alkalinity.

Table 4.3 Results from alkalinity test.

Sample	**Mass of additive/undiluted volume of inoculum used for test**	**Starting volume of test sample after water addition (ml)**	**Initial pH of test sample**	**Volume of acid consumed to pH 4.5 (ml)**	**Total alkalinity (mg $CaCO_3$/l)**
Synthetic graphite	5 g	100	6.1	0.1	2.5
Sludge biochar	5 g	100	7.8	2.05	40
Inoculum	50 ml	250	7.4	8.35	5219

Table 4.4 Normalised alkalinity in test reactors.

Sample	**Total alkalinity in mg $CaCO_3$/l**	**Normalised alkalinity**	**Alkalinity contribution in 150 ml test reactors**
SG	2.5	0.5 mg $CaCO_3$/l per g biochar	0.56 mg $CaCO_3$
SB	40	8 mg $CaCO_3$/l per g biochar	0.9 mg $CaCO_3$
Inoculum	5219	104.375 mg$CaCO_3$/l per ml inoculum	2348.4 mg $CaCO_3$

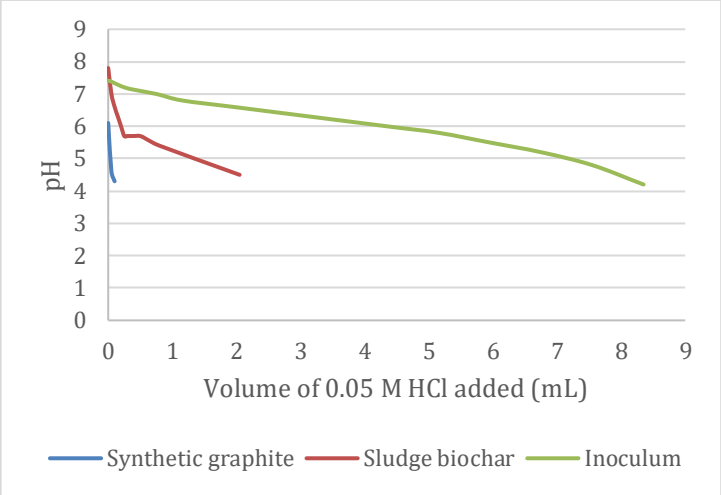

Figure 4.1 Observed decrease in pH in test samples during alkalinity test.

4.3 Electrical conductivity and pH test

Table 4.5 presents the results from the electrical conductivity and pH tests conducted on the reactor samples after the end of the experiment. Electrical conductivity values are indicative of dissolved salt concentration and can serve as a measure of sample salinity, with higher salt content correlating to increased electrical conductivity.

The results indicated relatively consistent electrical conductivity levels across the thermophilic reactor samples. Notably, Group B reactors exhibited lower electrical conductivity values compared to the other thermophilic reactors, potentially attributed to enhanced acetate ion degradation facilitated by the presence of sludge biochar.

In terms of final pH, thermophilic reactors in Groups A, B, and C demonstrated a more alkaline pH range between 8.2–8.3, in contrast to the room temperature reactor, which recorded a pH of 7.6. The blank reactor registered the lowest electrical conductivity value among the reactor groups, coupled with a pH of 7.9.

Table 4.5 Results from electrical conductivity and pH test on the reactor samples after the end of Phase 2 of the experiment

Reactor	**Electrical conductivity (milliSiemens/cm)**	**pH**
Group A (A1, A2, A3)	22.4 ± 0.2	8.3
Group B (B1, B2, B3)	21.7 ± 0.2	8.2
Group C (C1, C2, C3)	22.2 ± 0.1	8.2
Group D (D1, D2, D3)	19.1 ± 0.1	7.6
Blank (E)	2.32	7.9

4.4 Biogas production in Phase 1

Phase 1 of the experiment lasted for 26 days, from Day 0 to Day 25. At the end of Phase 1, the cumulative biogas yields (Mean ± SD) in the thermophilic reactor groups A, B, and C were measured at 1444.6 ± 41.3, 1436.0 ± 37.3, and 1414.7 ± 36.0 ml at STP, respectively. The measured pressure readings and the corresponding biogas volume in different test reactors has been presented in Appendix D.

Comparing the cumulative biogas yields in the thermophilic groups, there was not a significant difference between Groups A and B; however, both showed higher yields than the control Group C by approximately 2.1% and 1.5% respectively. This suggests a small positive effect due to the addition of additives in Group A and B reactors. Throughout Phase 1, the cumulative yield curves for all three reactors exhibited a similar trend. Group B demonstrated a slightly faster start-up and higher yields for the initial 10 days compared to Groups A and C (Figure 4.2).

Daily average biogas production rates in Groups A, B, and C exceeded 100 ml/day from Day 2 to Day 8, followed by a gradual decline (Figure 4.3). The peak daily average production rates for Groups A, B, and C were observed at 172.9, 156.9, and 155.4 ml/day, respectively, occurring on Day 4, Day 7, and Day 6 of the experiment.

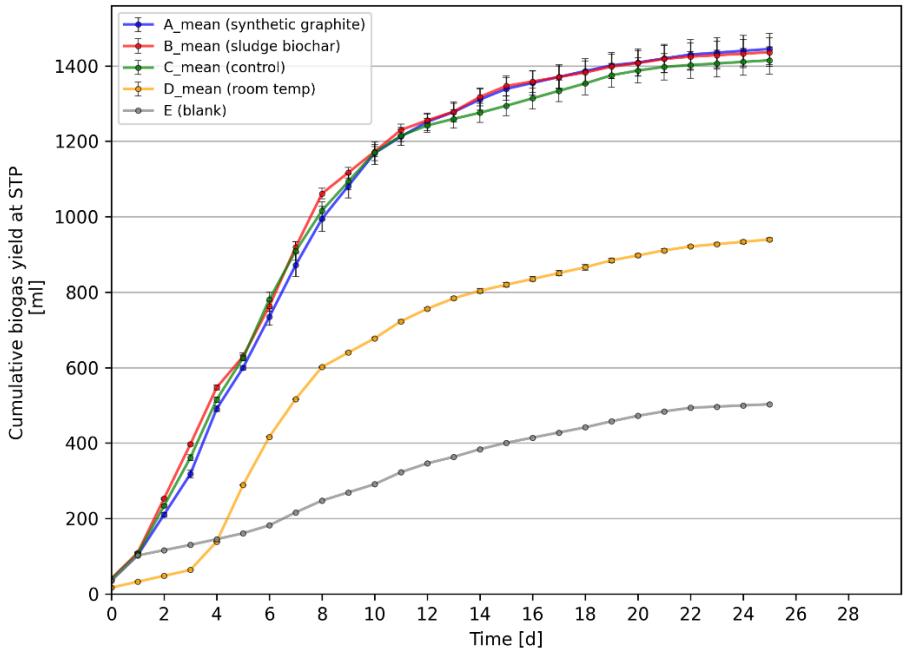

Figure 4.2 Cumulative biogas yield in different reactor groups during Phase 1 of the experiment. Error bars indicate standard deviation.

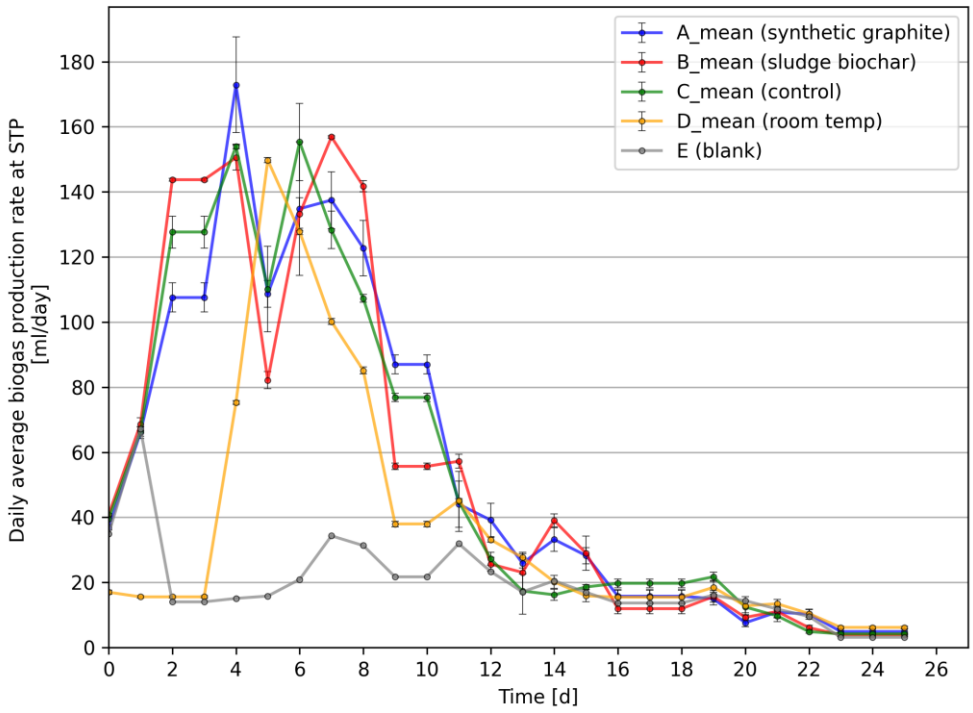

Figure 4.3 *Daily average biogas production in different reactor groups during Phase 1 of the experiment. Error bars indicate standard deviation.*

Group D, maintained at room temperature, showed a much lower cumulative biogas yield at the end of Phase 1, producing 939.7 ± 4.13 ml at STP, which was 33.6% less than the control C maintained at 55 °C. The average daily production rate for Group D was also considerably lower compared to the thermophilic reactors, with the highest average daily production of 149.8 ml/day recorded on Day 5. This difference could be attributed to the slower activity of methanogens at room temperature resulting in reduced methane production. Additionally, the lower temperature might have slowed down the hydrolysis and acidogenic reactions, leading to a delayed start-up of the digestion process.

The blank reactor E, maintained at 55 °C, yielded a cumulative biogas yield of 503 ml at STP at the end of Phase 1. This accounted for approximately 36% of the cumulative biogas yield in the control reactor C, representing the background biogas production in the thermophilic reactors. The average daily production rate in E remained low, ranging between 10 to 35 ml/day on all days except Day 1, where it peaked at 67.2 ml/day.

By deducting the background biogas production from the total biogas yields in the thermophilic reactor groups, the actual cumulative biogas yields in A, B, and C were calculated to be 941.7 ± 41.3, 933.1 ± 37.3, and 911.7 ± 36.0 ml at STP respectively. Comparing this with the theoretical biogas potential of 1.5 g microcrystalline cellulose, calculated to be 1244 ml at STP, the percentage degradation of substrate in reactor groups A, B, and C was approximately 76%, 75%, and 73%, respectively (Figure 4.4).

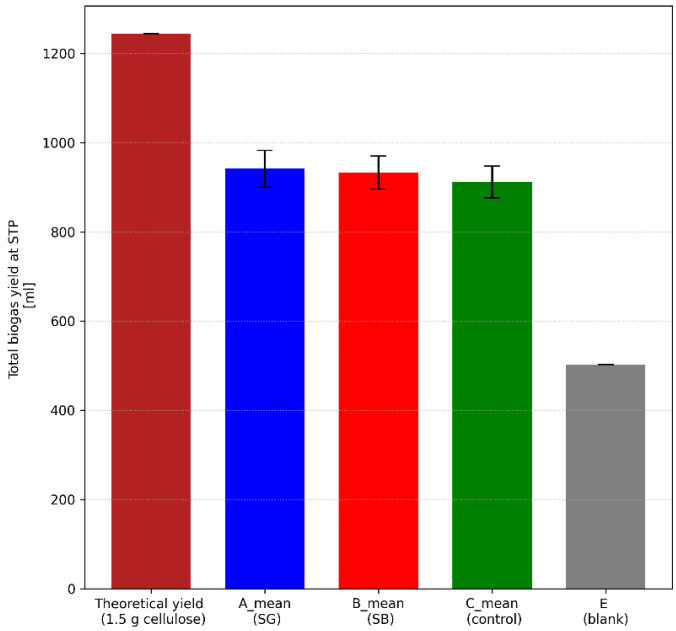

Figure 4.4 *Actual biogas yield in the thermophilic reactors in Phase 1 after deducting biogas background production. Error bars indicate standard deviation.*

4.5 Biogas production in Phase 2

The second phase of the experiment was started on Day 25 after the addition of 2.28 g of sodium acetate as the second substrate in reactor groups A, B, C and D. Phase 2 lasted for 23 days from Day 25 to Day 48 of the overall experiment. In contrast to Phase 1, which consisted of all four anaerobic digestion stages, digestion in Phase 2 consisted only of methanogenesis stage as sodium acetate readily dissolves in water to form acetate ions which is the main substrate for producing methane.

At the end of Phase 2, the cumulative biogas yield (Mean ± SD) in thermophilic reactor groups A, B and C was recorded at 710.2 ± 23.6, 790.8 ± 16.0 and 654.5 ± 26.4 ml at STP respectively (Figure 4.5). The measured pressure readings and the corresponding biogas volume in different test reactors has been presented in Appendix D. Notably, the final production in A and B surpassed that of the control by 8.51% and 20.82% respectively. Reactor B showed significantly higher daily average production rates for the first 7 days which were almost double than those in reactors A and C (Figure 4.6). However, B experienced a notable decline in daily production from Day 34 onwards, maintaining levels below 15 ml/day for the remainder of the experiment. Reactors A and C, on the other hand showed lower daily average production rates as compared to B, but they remained steady throughout the experiment period, dropping significantly only from Day 41 onwards. The presence of sludge biochar in B likely facilitated the accelerated conversion of acetate into methane by promoting syntropy between SAOB and hydrogenotrophic methanogens.

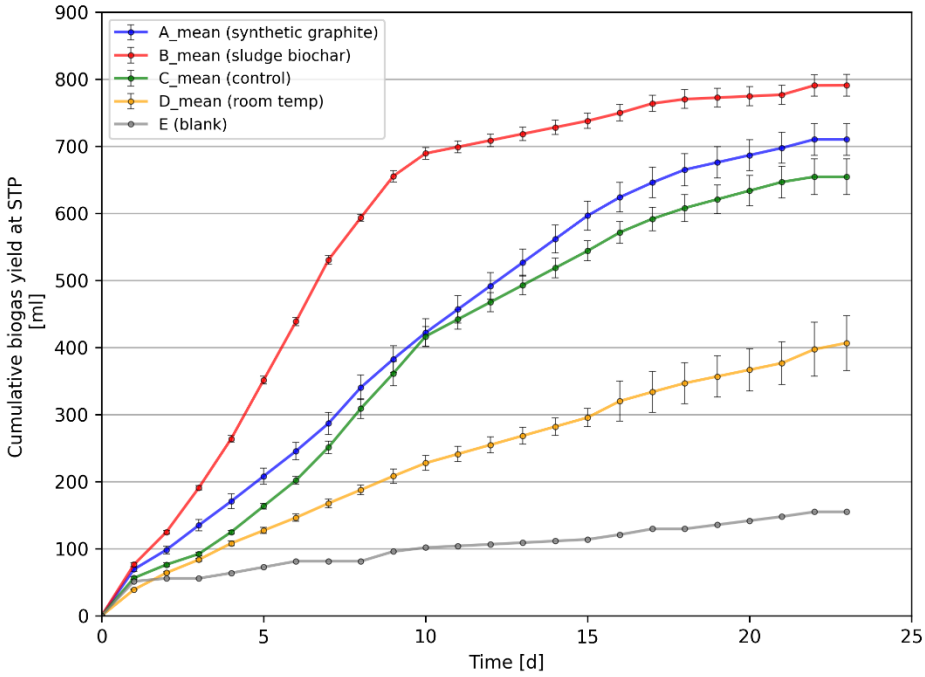

Figure 4.5 *Cumulative biogas yield in different reactor groups during Phase 2 of the experiment. Error bars indicate standard deviation.*

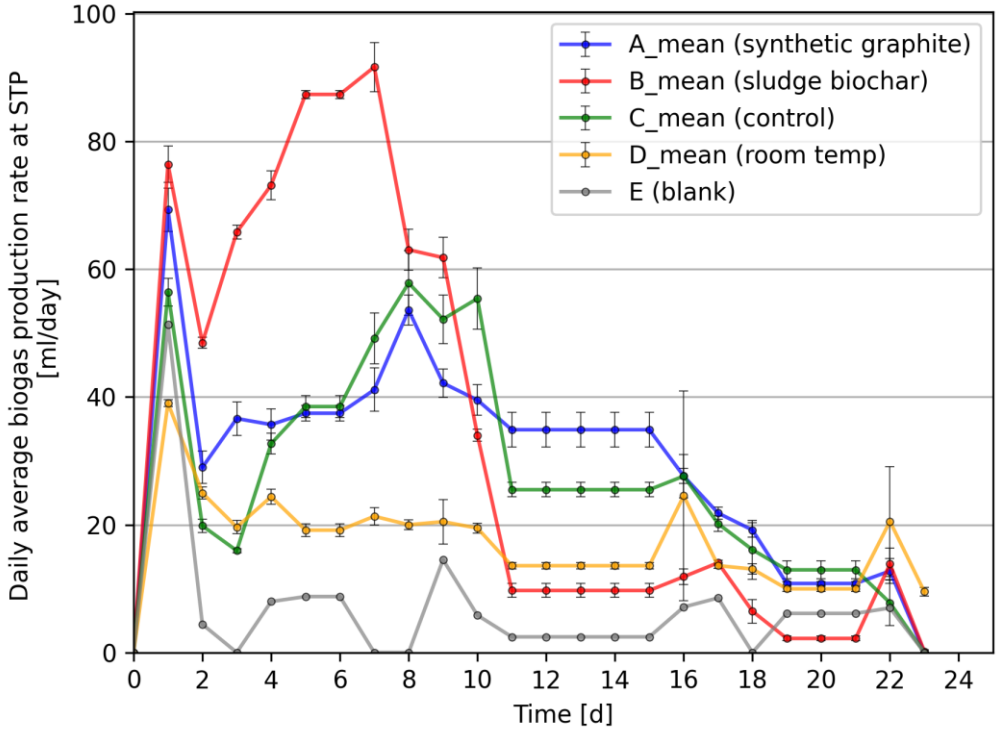

Figure 4.6 *Daily average biogas production in different reactor groups during Phase 2 of the experiment. Error bars indicate standard deviation.*

Reactor D showed a much lower cumulative yield at the end of Phase 2, producing 406.7 ± 40.86 ml of biogas. This was less than the production in the control reactor C by around 38%. The average daily production rate in Group D also lagged those in Groups A, B, and C, suggesting a slower digestion process at room temperature.

The blank reactor E, maintained at 55 °C, yielded a cumulative yield of 154.9 ml at the end of Phase 2, representing the background biogas production. This accounted for approximately 24% of the cumulative biogas yield in the control reactor C. The average daily production rate in E was much lower in Phase 2, staying below 10 ml/day for most of the experiment duration.

Deducting the production in blank reactor from the total cumulative yields in A, B and C, their actual biogas yields amounted to 555.3 ± 23.6, 636.0 ± 16.0 and 499.6 ± 26.4 ml respectively. Comparing this with the theoretical biogas potential of 2.28 g of sodium acetate, calculated to be 1246 ml at STP, the percentage degradation of substrate in reactors A, B and C was around 45%, 51% and 40% respectively (Figure 4.7). This percentage degradation of substrate was lower compared to Phase 1, possibly due to the higher water solubility of the produced HCO_3^- ions (Equation 2.13), resulting in lower headspace pressure due to biogas.

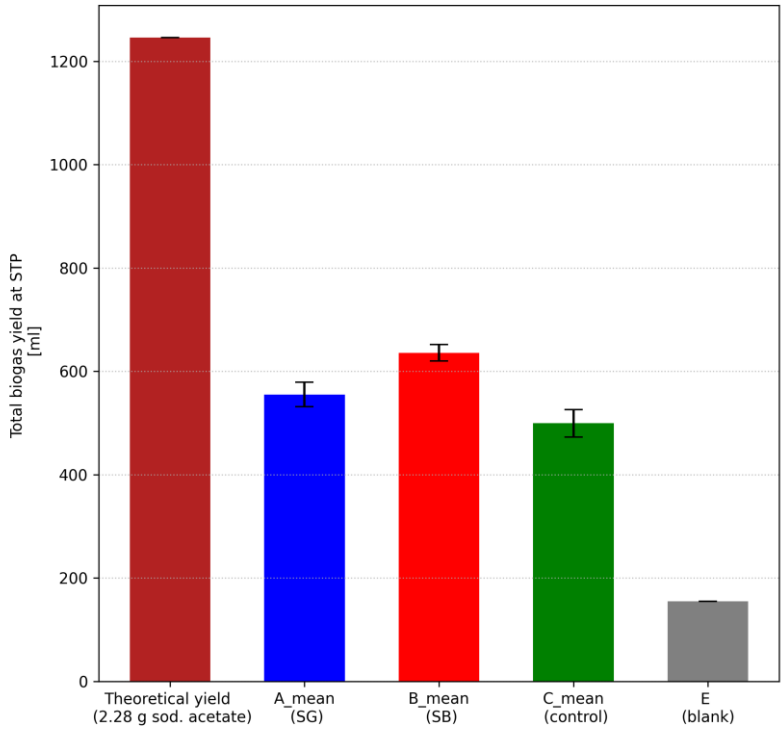

Figure 4.7 *Actual biogas yield in thermophilic reactors in Phase 2 after deducting background biogas production. Error bars indicate standard deviation.*

4.6 Combined biogas yield in both phases

The entire experiment, including both phases, ran for 49 days, starting on Day 0 and ending on Day 48. Phase 1 lasted from Day 0 to Day 25, while Phase 2 lasted from Day

25 to Day 48. The combined cumulative biogas production in reactor groups A, B and C totalled 2154.8 ± 57, 2226.9 ± 53.3 and 2069.1 ± 62.5 ml at STP respectively (Figure 4.8).

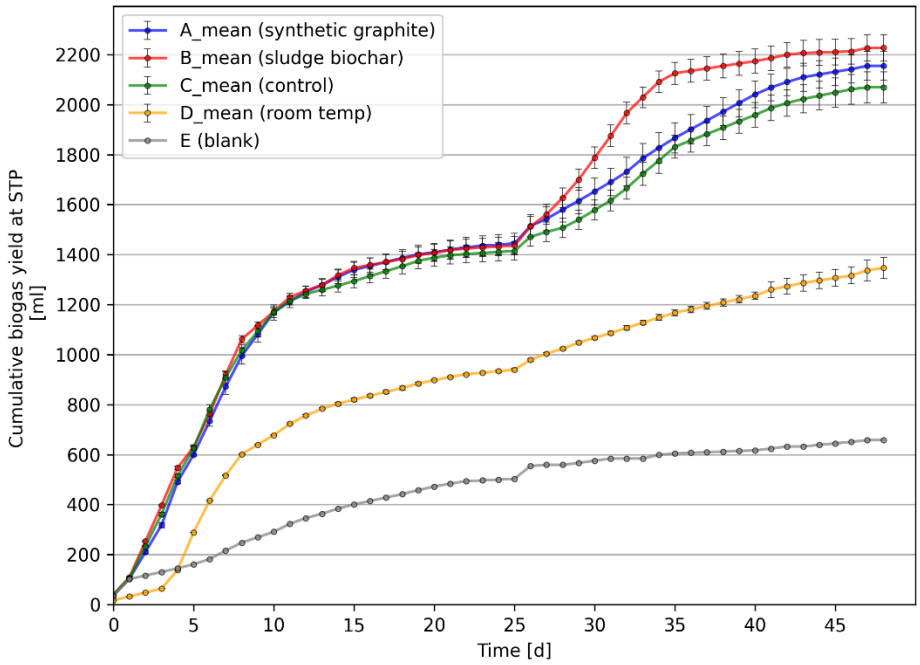

Figure 4.8 *Combined cumulative biogas yield during Phase 1 and Phase 2 of the experiment. Error bars indicate standard deviation.*

The combined total biogas production for both phases is presented in Table 4.6. It can be seen that the combined total yields in A and B, measured at 2154.8 ± 57 and 2226.9 ± 53.3ml respectively, surpassed that of control C by 4.14% and 7.62% respectively. Regarding the average daily production rate, there was not a big difference in reactors A, B and C in Phase 1. However, this shifted in Phase 2, where B exhibited a notably higher average daily production rate than A and C, resulting in an overall increased yield.

Table 4.6 Combined total biogas production in Phase 1 and Phase 2.

Reactor group	**Phase 1 (ml STP)**	**Phase 2 (ml STP)**	**Total (ml STP)**
Group A (SG)	1444.6 ± 41.3	710.2 ± 23.6	2154.8 ± 57
Group B (SB)	1436.0 ± 37.3	790.8 ± 16.0	2226.9 ± 53.3
Group C (control)	1414.7 ± 36.0	654.5 ± 26.4	2069.1 ± 62.5
E (blank)	503.0	154.9	657.8
E as % of C	35.5%	23.6%	31.8%
Group D (room temp)	939.7 ± 4.13	406.7 ± 40.86	1346.4 ± 42.6

The combined total biogas production in reactor D amounted to 1346.4 ± 42.6 ml, which was about 35% less compared to the control reactor C. Meanwhile, the blank reactor E yielded a combined total yield of 657.8 ml, roughly 32% of the combined total in the control reactor.

Deducting this background production from the combined total yields in A, B and C gave their actual combined yields of around 1497.0 ± 57.0, 1569.0 ± 53.3 and 1411.3 ± 62.5 ml respectively. Comparing this with the combined theoretical biogas potential of 1.5 g cellulose and 2.28 g of sodium acetate, calculated to be 2490.4 ml, the overall percentage degradation of both substrate in reactors A, B and C was around 60%, 63% and 57% respectively (Figure 4.9).

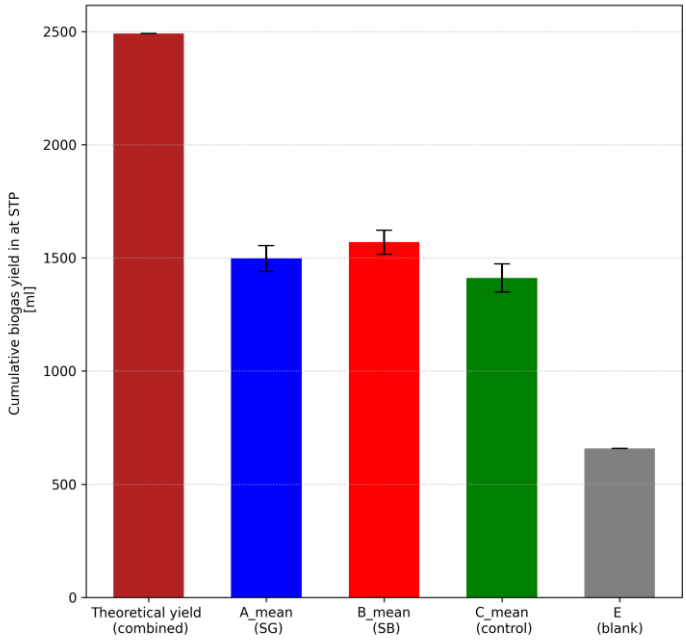

Figure 4.9 *Combined actual biogas yield in the thermophilic reactors in Phase 1 and Phase 2 after deducting background biogas production. Error bars indicate standard deviation.*

4.7 Statistical test results

Results from the one-way ANOVA test, with a 95% confidence interval, revealed statistically significant ($p < 0.05$) differences between the mean biogas production in A, B, and C on 17 out of 25 days during Phase 1. This indicated that biogas production in A and B was statistically different from that in the control. Results from Student's t-test (two-tailed, unequal variance, 95% confidence interval) comparing the daily biogas production in A and B with that in C indicated statistically significant ($p < 0.05$) differences between A and C on 9 out of 25 days and between B and C on 11 out of 25 days of Phase 1.

In Phase 2, the one-way ANOVA test showed statistically significant differences in mean biogas production among A, B, and C on 20 out of 23 days, indicating a stronger

effect of additive on biogas production compared to Phase 1. Similarly, results from Student's t-test comparing daily biogas production in A and B with that in C revealed statistically significant differences between A and C on 10 out of 23 days and between B and C on 18 out of 23 days of Phase 2.

The experiment used triplicate readings for each reactor group, with the exception of the blank reactor. However, this sample size was not sufficient to determine if the measured values followed a normal distribution. Nonetheless, no significant outliers were detected in any group's triplicate readings, confirmed through Dixon's test for single outliers.

Throughout the 48-day experiment, the coefficient of variation (CV) in daily readings for reactors A, B, C, and D remained below 10% for 32, 26, 36, and 38 days respectively, suggesting reliable measurements. When the permissible CV was increased to 15%, the readings were consistent on 43, 40, 43 and 45 days for each group. The higher CV in the readings could be attributed to the small size of the triplicate dataset for each group, which was not enough to reliably predict if they were normally distributed.

4.8 Possible mechanisms of stimulating biogas production from biochar

The potential mechanisms by which biochar can influence biogas production, as outlined in Section 2.5.1, include its influence on pH levels, VFA accumulation, overcoming ammonia inhibition, promoting the growth of beneficial microbes, and facilitating faster interspecies electron transfer. Results from the experiment indicate enhanced biogas yields in the SB dosed reactors compared to the control group. The increase in biogas yield due to SB was more significant in Phase 2 than in Phase 1. In Phase 1, the yield exceeded that of the control reactors by 2.1%, while in Phase 2, it exceeded the control reactors by 20.8%.

The first phase of the experiment, using microcrystalline cellulose as substrate, likely underwent all four stages of anaerobic digestion, including the production and conversion of VFAs in the acidogenesis and acetogenesis stages. However, since no VFA analysis was conducted, understanding the effect of SB on VFA production and conversion is difficult. Nonetheless, the 2.1% higher biogas production could likely be attributed to enhanced VFA conversion efficiency due to the presence of biochar.

Regarding reactor alkalinity, which is essential for maintaining optimal pH and good buffer capacity in the digester, over 99% of the alkalinity was contributed by the inoculum in both phases. However, SB exhibited higher alkalinity compared to SG, suggesting its potential to improve buffering capacity at higher concentrations, thereby maintaining an optimal pH and improving VFA conversion efficiency.

In the second phase of the experiment, sodium acetate was used, a compound that readily dissolves in water to produce acetate, thereby triggering only the methanogenesis stage of anaerobic digestion. Biogas yield in this phase saw an increase of around 20.8% compared to the control.

This increase could be attributed to the higher water solubility of sodium acetate in contrast to the insolubility of microcrystalline cellulose. The acetate so produced could have reached the microorganisms in the biochar pores more easily facilitating its degradation. Additionally, the larger specific surface area of sludge biochar could have

resulted in an increased growing area for the microorganisms, potentially contributing to the increased biogas yield. Moreover, the micro and mesopores present on the biochar surface could have facilitated the functional enrichment of the microbial community, thereby accelerating the methanogenesis reactions. Performing a microbial analysis could offer better insight into the abundance and diversity of microorganisms in the different reactor groups.

Dyksma et al. (2020) observed that under thermophilic conditions and with high acetate concentrations, syntrophic acetate oxidation followed by hydrogenotrophic methanogenesis (SAO-HM) can become the dominant methanogenesis pathway. The efficiency of this two-step pathway depends on the efficient utilisation of the hydrogen produced by SAOB by hydrogenotrophic methanogens. SB could have played a role in enhancing this collaboration between the two microbial groups, potentially facilitating a faster interspecies electron transfer between them. However, confirmation of this hypothesis would require additional analysis of the reactor samples, which was not possible within the short timeframe of this thesis project.

The effect of SB on ammonia inhibition could not be assessed in the experiment since both test substrates lacked nitrogen, resulting in no ammonia production in the reactors. Conducting the same experiment using nitrogenous substrates like WAS or food waste could help elucidate the effect of SB on ammonia inhibition. Similarly, physiochemical analysis of the SB was not conducted, which could have provided a better understanding of its chemical composition, presence of functional groups, specific surface area and adsorption capacity. Additionally, performing VFA analysis and microbial analysis on reactor samples at different stages could provide insight into the VFA concentrations and different groups of microorganisms present in each reactor. Such analyses could be considered in future studies to gain a better understanding of SB's effect on the anaerobic digestion process.

5 Conclusion

This thesis aimed to investigate the effect of sludge biochar as an additive in thermophilic anaerobic digestion of easily biodegradable substrates by examining its impact on biogas production.

In the first phase of the experiment, which used microcrystalline cellulose as the substrate, the addition of SB resulted in a small increase in biogas yield. Reactors with SB and SG additives produced only 1.5% and 2.1% more biogas, respectively, compared to control reactors without any additives.

In the second phase, which used sodium acetate as the substrate, a significant difference in biogas production was observed among the reactor groups. Reactors with SB and SG additives produced 21% and 8.5% more biogas, respectively, compared to the control group. This finding highlights the potential of sludge biochar to improve thermophilic anaerobic digestion performance, especially in environments where SAO-HM is the dominant methanogenesis pathway. However, additional investigations are necessary to gain a better understanding of the enhancement mechanism and its applicability with complex substrates like sewage sludge.

In contrast, biogas production in Group D reactors, maintained at room temperature, remained consistently low across both phases. These reactors produced 35% less biogas in Phase 1 and 25% less in Phase 2 compared to the control, indicating slower substrate degradation and microbial inactivity at lower temperatures.

5.1 Future studies and recommendations

Given the constraints of time for both the literature review and laboratory experiments in this thesis project, the following recommendations are proposed for future research:

- Compare digestion performance at mesophilic and thermophilic temperatures.
- Perform the experiment with different substrates, varied inoculum to substrate ratios, and different additive concentrations.
- Perform gas chromatography to determine the proportions of methane and carbon dioxide in the produced biogas.
- Perform VFA analysis to evaluate digestion performance at different stages of the experiment.
- Perform microbial analysis to understand the impact of SB on the diversity and abundance of microorganisms.

6 References

Agrafioti, E., Bouras, G., Kalderis, D., & Diamadopoulos, E. (2013). Biochar production by sewage sludge pyrolysis. *Journal of Analytical and Applied Pyrolysis, 101*. doi:http://dx.doi.org/10.1016/j.jaap.2013.02.010

Ambaye, T., Rene, E., Wongrod, S., & Van Hullebusch, E. (2020). Anaerobic Digestion of Fruit Waste Mixed With Sewage Sludge Digestate Biochar: Influence on Biomethane Production. *Frontiers in Energy Research, 8*. doi:10.3389/fenrg.2020.00031

Angelidaki, I., Alves, M., Bolzonella, D., Borzacconi, L., Campos, J., Guwy, A., . . . van Lier, J. (2009). Defining the biomethane potential (BMP) of solid organic wastes and energy crops: a proposed protocol for batch assays. *Water Science and Technology, 59*(5), 927–934. doi:https://doi.org/10.2166/wst.2009.040

APHA. (2017). *Standard Methods for the Examination of Water and Wastewater (23rd ed.).* Washington DC: American Public Health Association.

Appels, L., Baeyens, J., Degreve, J., & Dewil, R. (2008). Principles and potential of the anaerobic digestion of waste-activated sludge. *Progress in Energy and Combustion Science, 34*, 755-781. doi:https://doi.org/10.1016/j.pecs.2008.06.002

Baek, G., Kim, J., Kim, J., & Lee , C. (2018). Role and Potential of Direct Interspecies Electron Transfer in Anaerobic Digestion. *Energies, 11*(1), 107. doi:https://doi.org/10.3390/en11010107

Boyle, W. (1977). Energy recovery from sanitary landfills - A review. *Microbial Energy Conversion: The Proceedings of a Seminar Sponsored by the UN Institute for Training and Research (UNITAR) and the Ministry for Research and Technology of the Federal Republic of Germany Held in Göttingen, October 1976.* doi:https://doi.org/10.1016/B978-0-08-021791-8.50019-6

Buswell, A., & Mueller, H. (1952). Mechanism of Methane Fermentation. *Industrial and Engineering Chemistry, 44*(3), 550-552. doi:https://doi.org/10.1021/ie50507a033

Chen , G., van Loosdrecht, M. C., Ekama, G., & Brdjanovic , D. (2020). *Biological Wastewater Treatment: Principles, Modelling and Design.* London: IWA Publishing. Retrieved 02 08, 2024, from https://iwaponline.com/ebooks/book/791/Biological-Wastewater-TreatmentPrinciples

Conrad, R. (2020). Importance of hydrogenotrophic, aceticlastic and methylotrophic methanogenesis for methane production in terrestrial, aquatic and other anoxic environments: A mini review. *Pedosphere, 30*(1), 25-39. doi:https://doi.org/10.1016/S1002-0160(18)60052-9

Dagerskog, L., & Olsson, O. (2020). *Swedish sludge management at the crossroads (Policy brief).* Stockholm Environment Institute. Retrieved 02 06, 2024, from https://www.sei.org/publications/swedish-sludge-crossroads/

Dang, Y., Holmes, D. E., Zhao, Z., Woodard, T. L., Zhang, Y., Sun, D., . . . Lovley, D. R. (2016). Enhancing anaerobic digestion of complex organic waste with carbon-based conductive materials. *Bioresource Technology, 220*, 516-522. doi:https://doi.org/10.1016/j.biortech.2016.08.114

De la Rubia, M. A., Riau, V., Raposo, F., & Borja, R. (2013). Thermophilic anaerobic digestion of sewage sludge: focus on the influence of the start-up. A review. *Critical Reviews in Biotechnology, 33*(4), 448-460. doi:https://doi.org/10.3109/07388551.2012.726962

Deublein, D., & Steinhauser, A. (2008). *Biogas from Waste and Renewable Resources: An Introduction.* Weinheim: Wiley-VCH Verlag GmbH & Co. KGaA. doi:DOI:10.1002/9783527621705

Djandja, O., Wang, Z.-C., Wang, F., Xu, Y.-P., & Duan, P.-G. (2020). Pyrolysis of Municipal Sewage Sludge for Biofuel Production: A Review. *Industrial and Engineering Chemistry Research, 59*(39), 16939–16956. doi:https://doi.org/10.1021/acs.iecr.0c01546

Dyksma, S., Jansen, L., & Gallert, C. (2020). Syntrophic acetate oxidation replaces acetoclastic methanogenesis during thermophilic digestion of biowaste. *Microbiome, 8*(105). doi:https://doi.org/10.1186/s40168-020-00862-5

EurEau. (2021). *Waste water treatment - sludge management (Briefing note).* European Federation of National Associations of Water Services. Retrieved 02 06, 2024, from https://www.eureau.org/resources/briefing-notes/5629-briefing-note-on-sludge-management/file

Ferrer, I., Vazquez, F., & Font, X. (2011). Comparison of the Mesophilic and Thermophilic Anaerobic Sludge Digestion from an Energy Perspective. *Journal of Residuals Science & Technology, 8*(2). Retrieved from https://core.ac.uk/download/pdf/157808586.pdf

Foladori, P., Andreottola, G., & Giuliano, Z. (2010). *Sludge Reduction Technologies in Wastewater Treatment Plants.* IWA Publishing. doi:https://doi.org/10.2166/9781780401706

Fransson, A., Gustafsson, M., Malmberg, J., & Paulsson, M. (2020). *The Biochar Handbook – for users (English translation of the Swedish handbook - Biokolhandboken – för användare).* Region Skåne and Vinnova. Retrieved from https://biokol.org/publikationer/pdf/biochar-handbook-for-users

Gaur, A., & Bardiya, N. (1997). Effects of carbon and nitrogen ratio on rice straw biomethanation. *J. Rural Energy, 4*((1-4)), 1-16.

Gebreeyessus, G. D., & Jenicek, P. (2016). Thermophilic versus Mesophilic Anaerobic Digestion of Sewage Sludge: A Comparative Review. *Bioengineering, 3*(15). doi:doi:10.3390/bioengineering3020015

Gustafsson, M., & Anderberg, S. (2023). Great expectations—future scenarios for production and use of biogas and digestate in Sweden. *Biofuels, 14*(1), 93-107. doi:10.1080/17597269.2022.2121543

Harirchi, S., Wainainaa, S., Sar, T., Nojoumi, S. A., Parchami, M., Parchami, M., . . . Taherzadeh, M. J. (2022). Microbiological insights into anaerobic digestion for biogas, hydrogen or volatile fatty acids (VFAs): a review. *Bioengineered, 13*(3), 6521-6557. doi: https://doi.org/10.1080/21655979.2022.2035986

Holliger, C., Alves, M., Andra, D., Angelidaki, I., & Astals, S. (2016). Towards a standardization of biomethane potential tests. *Water Science Technology, 74*(11), 2515-2522. doi:doi: 10.2166/wst.2016.336

Holohan, B. C., Duarte, M. S., Szabo-Corbacho, A. M., Cavaleiro, J. A., Salvador, A. F., Pereira, M. A., . . . Alves, M. M. (2022). Principles, Advances, and Perspectives of Anaerobic Digestion of Lipids. *Environmental Science and Technology, 56*(8), 4749-4775. doi:https://doi.org/10.1021/acs.est.1c08722

Huggins, T. M., Haeger, A., Biffinger, J. C., & Ren, Z. J. (2016). Granular biochar compared with activated carbon for wastewater treatment and resource recovery. *Water Research, 94*, 225-232. doi:https://doi.org/10.1016/j.watres.2016.02.059

Kardos, L., Juhasz, A., Palko, G. Y., Olah, J., Barkacs, K., & Zaray, G. Y. (2011). Comparing of mesophilic and thermophilic anaerobic fermented sewage

sludge based on chemical and biochemical tests. *Applied Ecology and Environmental Research, 9*(3). doi:DOI:10.15666/AEER/0903_293302

Khoei, S., Stokes, A., Kieft, B., Kadota, P., Hallam, S. J., & Eskicioglu, C. (2021). Biochar amendment rapidly shifts microbial community structure with enhanced thermophilic digestion activity. *Bioresource Technology, 341*, 125864. doi:https://doi.org/10.1016/j.biortech.2021.125864

Koch, K., Hafner, S., Weinrich, S., Astals, S., & Holliger, C. (2020). Power and Limitations of Biochemical Methane Potential (BMP) Tests. *Frontiers in Energy Research, 8*. doi:https://doi.org/10.3389/fenrg.2020.00063

Koukouzas, N., Hämäläinen, J., Papanikolaou, D., Tourunen, A., & Jäntti, T. (2007). Mineralogical and elemental composition of fly ash from pilot scale fluidised bed combustion of lignite, bituminous coal, wood chips and their blends. *Fuel, 86*(14), 2186-2193. doi:https://doi.org/10.1016/j.fuel.2007.03.036

Labatut, R. A., Angenent, L. T., & Norman, R. S. (2014). Conventional mesophilic vs. thermophilic anaerobic digestion: A trade-off between performance and stability? *Water Research, 53*, 249-258. doi:https://doi.org/10.1016/j.watres.2014.01.035

Lanko, I. (2021). Comparison of the mesophilic, thermophilic and temperature-phased anaerobic digestion of sewage sludge (Ph.D. dissertation). Department of Water Technology and Environmental Engineering, University of Chemistry and Technology, Prague & Department of Civil and Environmental Engineering, Universitat Politècnica de Catalunya (BarcelonaTech), Spain. Retrieved from http://hdl.handle.net/10803/674732

Li, Q., Xu, M., Wang, G., Chen, R., Qiao, W., & Wang, X. (2018). Biochar assisted thermophilic co-digestion of food waste and waste activated sludge under high feedstock to seed sludge ratio in batch experiment. *Bioresource Technology, 249*, 1009-1016. doi:https://doi.org/10.1016/j.biortech.2017.11.002

Meegoda, J. N., Li, B., Patel, K., & Wang, L. B. (2018). A Review of the Processes, Parameters, and Optimization of Anaerobic Digestion. *International Journal of Environmental Research and Public Health, 15*(10), 2224. doi:https://doi.org/10.3390/ijerph15102224

Menzel, T., Neubauer, P., & Junne, S. (2020). Role of Microbial Hydrolysis in Anaerobic Digestion. *Energies, 13*(21), 5555. doi:https://doi.org/10.3390/en13215555

Metcalf & Eddy, Tchobanoglous, G., Stensel, H. D., Tsuchihashi, R., & Burton, F. (2014). *Wastewater Engineering: Treatment and Resource Recovery (5th ed.).* McGraw-Hill.

Mosbaek, F., Kjeldal, H., Mulat, D., Albertsen, M., Ward, A., Feilberg, A., & Nielsen, J. (2016). Identification of syntrophic acetate-oxidizing bacteria in anaerobic digesters by combined protein-based stable isotope probing and metagenomics. *International Society for Microbial Ecology (ISME) Journal, 10*(10), 2405–2418. doi:https://doi.org/10.1038/ismej.2016.39

Muzenda, E. (22-24 October 2014). Bio-methane Generation from Organic Waste: A Review. *Proceedings of the World Congress on Engineering and Computer Science.* San Francisco, USA. Retrieved from https://www.iaeng.org/publication/WCECS2014/WCECS2014_pp647-652.pdf

Owen, W., Stuckey, D., Healy Jr., J., Young, L., & McCarty, P. (1979). Bioassay for monitoring biochemical methane potential and anaerobic toxicity. *Water Research, 13*(6). doi:https://doi.org/10.1016/0043-1354(79)90043-5

Pan, J., Ma, J., Zhai, L., Luo, T., Mei, Z., & Liu, H. (2019). Achievements of biochar application for enhanced anaerobic digestion: A review. *Bioresource Technology, 292*. doi:https://doi.org/10.1016/j.biortech.2019.122058

Persson, T. (2012). *Final report on the Swedish participation in Task 37 of the International Energy Agency (SGC Rapport 2012:268).* Svenskt Gasteknik Center (SGC). Retrieved January 22, 2024, from http://www.sgc.se/ckfinder/userfiles/files/SGC268.pdf

Plante, A., Stone, M., & McGil, W. (2015). Chapter 9: The Metabolic Physiology of Soil Microorganisms. In E. Paul, *Soil Microbiology, Ecology and Biochemistry (Fourth Edition)* (pp. 245-272). Academic Press. doi:https://doi.org/10.1016/B978-0-12-415955-6.00009-8

Qadir, M., Drechsel, P., Cisneros, B. J., Kim, Y., Amit, P., Praem, M., & Oluwabusola, O. (2020). Global and regional potential of wastewater as a water, nutrient and energy source. *Natural Resources Forum, 44*, 40-51. doi:DOI: 10.1111/1477-8947.12187

Qiu, L., Deng, Y., Wang, F., Davaritouchaee, M., & Yao, Y. (2019). A review on biochar-mediated anaerobic digestion with enhanced methane recovery. *Renewable and Sustainable Energy Reviews, 115*. doi:https://doi.org/10.1016/j.rser.2019.109373

Rajagopal, R., Massé, D. I., & Singh, G. (2013). A critical review on inhibition of anaerobic digestion process by excess ammonia. *Bioresource Technology, 143*, 632-641. doi:https://doi.org/10.1016/j.biortech.2013.06.030

Sarker, S., Lamb, J. J., Hjelme, D. R., & Lien, K. M. (2019). A Review of the Role of Critical Parameters in the Design and Operation of Biogas Production Plants. *Applied Sciences, 9*(9), 1915. doi:https://doi.org/10.3390/app9091915

Schnürer, A., & Jarvis, Å. (2018). *Microbiology of the biogas process.* Swedish University of Agricultural Sciences. Retrieved from https://res.slu.se/id/publ/98208

Schnürer, A., & Nordberg, A. (2008). Ammonia, a selective agent for methane production by syntrophic acetate oxidation at mesophilic temperature. *Water Science Technology, 57*(5), 735-740. doi:doi: 10.2166/wst.2008.097

SEPA. (2012). *Biogas from manure, waste and residual products – Good Swedish examples (Biogas ur gödsel, avfall och restprodukter – Goda svenska exempel).* Stockholm: Naturvårdsverket. Retrieved January 22, 2024, from https://www.diva-portal.org/smash/get/diva2:1614170/FULLTEXT01.pdf

Sharma, P., & Melkania, U. (2017). Biochar-enhanced hydrogen production from organic fraction of municipal solid waste using co-culture of Enterobacter aerogenes and E. coli. *International Journal of Hydrogen Energy, 42*(30), 18865-18874. doi:https://doi.org/10.1016/j.ijhydene.2017.06.171

Shen, Y., Linville, J. L., Urgun-Demirtas, M., Schoene, R. P., & Snyder, S. W. (2015). Producing pipeline-quality biomethane via anaerobic digestion of sludge amended with corn stover biochar with in-situ CO2 removal. *Applied Energy*, 300-309. doi:https://doi.org/10.1016/j.apenergy.2015.08.016

Sossa, K., Alarcón, M., Aspé, E., & Urrutia, H. (2004). Effect of ammonia on the methanogenic activity of methylaminotrophic methane producing Archaea enriched biofilm. *Anaerobe, 10*(1), 13-18. doi:https://doi.org/10.1016/j.anaerobe.2003.10.004

Su, K., Li, L., Wang, Q., & Cao, R. (2023). A Review on the Interspecies Electron Transfer of Methane Production in Anaerobic Digestion System. *Fermentation, 9*(5), 467. doi:https://doi.org/10.3390/fermentation9050467

Sun, C., Guo, L., Zhenga, Y., Yu, D., Jin, C., Zhao, Y., . . . She, Z. (2021). The hydrolysis and reduction of mixing primary sludge and secondary sludge with thermophilic bacteria pretreatment. *Process Safety and Environmental Protection, 156*, 288-294. doi:https://doi.org/10.1016/j.psep.2021.10.026

Sweden Water Research. (2024, March 22). *Testbed Ellinge*. Retrieved from https://www.swedenwaterresearch.se/en/projekt/testbed-ellinge/

Tan, C., Yaxin, Z., Hongtao, W., Wenjing, L., Zeyu, Z., Yuancheng, Z., & Lulu, R. (2014). Influence of pyrolysis temperature on characteristics and heavy metal adsorptive performance of biochar derived from municipal sewage sludge. *Bioresource Technology, 164*, 47–54. doi:http://dx.doi.org/10.1016/j.biortech.2014.04.048

Tang, S., Wang, Z., Liu, Z., Zhang, Y., & Si, B. (2020). The Role of Biochar to Enhance Anaerobic Digestion: A Review. *Journal of Renewable Materials, 8*(9). doi:https://doi.org/10.32604/jrm.2020.011887

Uddin, M., & Wright, M. M. (2021). Anaerobic digestion fundamentals, challenges, and technological advances. *Physical Sciences Reviews, 8*(9). doi:https://doi.org/10.1515/psr-2021-0068

VDI 4630. (2016). *Fermentation of organic materials – characterization of the substrate, sampling, collection of material data, fermentation tests.* Verlag des Vereins Deutscher Ingenieure. Retrieved from https://www.vdi.de/richtlinien/details/vdi-4630-fermentation-of-organic-materials-characterization-of-the-substrate-sampling-collection-of-material-data-fermentation-tests

Wainaina, S., Lukitawesa, Kumar, A. M., & Taherzadeh, M. (2019). Bioengineering of anaerobic digestion for volatile fatty acids, hydrogen or methane production: a critical review. *Bioengineered, 10*, 437-458. doi:10.1080/21655979.2019.1673937

Wang, B., Nges, I., Nistor, M., & Liu, J. (2014). Determination of methane yield of cellulose using different experimental setups. *Water Science and Technology, 70*(4), 599-604. doi:https://doi.org/10.2166/wst.2014.275

Wang, G., Li, Q., Dzakpasu, M., Gao, X., Yuwen, C., & Wang, X. C. (2018). Impacts of different biochar types on hydrogen production promotion during fermentative co-digestion of food wastes and dewatered sewage sludge. *Waste Management, 80*, 73-80. doi:https://doi.org/10.1016/j.wasman.2018.08.042

Wang, T., Zhai, Y., Zhu, Y., Li, C., & Zeng, G. (2018). A review of the hydrothermal carbonization of biomass waste for hydrochar formation: Process conditions, fundamentals, and physicochemical properties. *Renewable and Sustainable Energy Reviews, 90*, 223-247. doi:https://doi.org/10.1016/j.rser.2018.03.071

Weinrich, S., Schäfer, F., Bochmann, G., & Liebetrau, J. (2018). *Value of batch tests for biogas potential analysis; method comparison and challenges of substrate and efficiency evaluation of biogas plants.* International Energy Agency (IEA) Bioenergy. IEA Bioenergy Task 37. Retrieved from https://task37.ieabioenergy.com/wp-content/uploads/sites/32/2022/02/Batch_tests_web_END.pdf

Weissbach, F. (2009). Evaluation of the renewable primary products for biogas production. Part I: Gas production potential of the fermentable nutrients. *Pflanzenbauwissenschaften, 13*(2), 72-85. Retrieved from https://www.openagrar.de/receive/openagrar_mods_00048500

Wu, B., Yang, Q., Yao, F., Chen, S., He, L., Hou, K., . . . Li, X. (2019). Evaluating the effect of biochar on mesophilic anaerobic digestion of waste activated

sludge and microbial diversity. *Bioresource Technology, 294*, 122235. doi:https://doi.org/10.1016/j.biortech.2019.122235

Xie, S., Li, X., Wang, C., Kulandaivelu, J., & Jiang, G. (2020). Enhanced anaerobic digestion of primary sludge with additives: Performance and mechanisms. *Bioresource Technology, 316*. doi:https://doi.org/10.1016/j.biortech.2020.123970

Zhang, D., Li, W., Hou, C., Shen, J., Jiang, X., Sun, X., . . . Liu, X. (2017). Aerobic granulation accelerated by biochar for the treatment of refractory wastewater. *Chemical Engineering Journal*, 88-97. doi:https://doi.org/10.1016/j.cej.2016.12.128

Zhang, M., Li, J., Wang, Y., & Yang, C. (2019). Impacts of different biochar types on the anaerobic digestion of sewage sludge. *RSC Advances*(72). doi:https://doi.org/10.1039/C9RA08700A

Appendix A

Calculation of initial dose for inoculum, substrate and additives

a) Inoculum dose

Assumed VS (w/w%) of inoculum based on previous year data from Ryaverket WWTP = 2%

Adopted inoculum volume per reactor = 150 ml

Resulting concentration of inoculum per reactor = 0.02*150 = 3 g VS

b) Substrate dose

Assumed VS (w/w%) content of microcrystalline cellulose = ≥ 99%

Assumed VS (w/w%) content of anhydrous sodium acetate = ≥ 99%

Adopted inoculum to substrate ratio (ISR) = 2:1

Phase 1: Microcrystalline cellulose dose per reactor

= 0.5*3 (based on adopted ISR value)

= 1.5 g VS

Molecular weight of cellulose ($C_6H_{10}O_5$)= 6*12 + 10*1 + 5*16
= 72 + 10 + 80
= 162 g/mol

Carbon content in 1.5 g cellulose = (72/165) * 1.5
= 0.67 g

Phase 2: Anhydrous sodium acetate

Molecular weight of sodium acetate (CH_3COONa)

= 2*12 + 3*1 + 2*16 + 23
= 24 + 3 + 32 +23
= 82 g/mol

Sodium acetate dose per reactor

= 0.67 * (82/24) (to maintain the same carbon content as in Phase 1)
= 2.28 g

c) Additive dose

7.5 g of additive added per reactor to maintain a high additive concentration of 50 g/l.

Appendix B

a) Sample calculation to calculate number of moles of produced biogas using measured headspace pressure

Reactor volume (equal to empty headspace volume)	= 0.00017321	m^3	(constant)
Reactor temperature for Setup 1 reactors (55 °C)	= 328.15	K	(constant)
Reactor temperature for Setup 2 reactors (21 °C)	= 294.15	K	(constant)
Universal gas constant (R)	= 8.314	Pa-m^3/mol.K	
Measured headspace pressure in reactor B1 on Day 3	= 156.6 kPa		(variable)
Measured headspace pressure in reactor D1 on Day 5	= 93.7	kPa	(variable)

Ideal gas equation: $PV = nRT$

$$n = \frac{PV}{RT}$$

Calculated number of moles of biogas produced in reactor B1 on Day 3
= (156600 * 0.00017321) / (8.314 * 328.15)
= 0.00995 moles

Calculated number of moles of biogas produced in reactor D1 on Day 5
= (93700 * 0.00017321) / (8.314 * 328.15)
= 0.00664 moles

b) Sample conversion of the calculated number of moles of biogas to biogas volume at STP conditions

Reactor volume (equal to empty headspace volume)	= 0.00017321	m^3	(constant)
Standard temperature (T)	= 273.15	K	(constant)
Standard pressure (P)	=101.325	kPa	(constant)
Universal gas constant (R)	= 8.314	Pa-m^3/mol.K	
Calculated number of moles in reactor B1 on Day 3	= 0.00995	moles	(variable)
Calculated number of moles in reactor D1 on Day 5	= 0.00664	moles	(variable)

Ideal gas equation: $PV = nRT$

$$V = \frac{nRT}{P}$$

Calculated biogas volume (STP) in reactor D1 on Day 5
= (0.00995 * 8.314 * 273.15) / 101325
= 0.000223 m^3
= 223 ml

Calculated biogas volume (STP) in reactor D1 on Day 5
= (0.00664 * 8.314 * 273.15) / 101325
= 0.000148 m^3
= 148.8 ml

Appendix C

Calculation of theoretical biogas yield of substrates

Phase 1: Microcrystalline cellulose ($C_6H_{10}O_5$)

Based on model by Buswell & Mueller (1952):

$$C_aH_bO_c + \left(a - \frac{b}{4} - \frac{c}{2}\right) H_2O \rightarrow \left(\frac{a}{2} - \frac{b}{8} + \frac{c}{4}\right) CO_2 + \left(\frac{a}{2} + \frac{b}{8} - \frac{c}{4}\right) CH_4$$

For cellulose, ***a =6, b =10, c =5***

$$C_6H_{10}O_5 + \left(6 - \frac{10}{4} - \frac{5}{2}\right) H_2O \rightarrow \left(\frac{6}{2} - \frac{10}{8} + \frac{5}{4}\right) CO_2 + \left(\frac{6}{2} + \frac{10}{8} - \frac{5}{4}\right) CH_4$$

$$C_6H_{10}O_5 + H_2O \rightarrow 3CO_2 + 3CH_4$$

1 mole cellulose → 3 moles methane
162 g cellulose → 3 moles methane

Using ideal gas equation: $V = \frac{nRT}{P}$

162 g cellulose → $\frac{3*8.314*273.15}{101.325}$ = *67.238 m^3* = 67238 ml at STP

1 g cellulose → $\frac{67.238}{162}$ = 0.415 *m^3* = 415 ml at STP

Since the molar ratio for CO_2 and CH_4 is 3:3, the gas composition is 50% CO_2 and 50% CH_4

Thus, the theoretical biogas yield (methane + carbon dioxide) of cellulose
= 2 * 415 ml/ g VS = 830 ml/g VS at STP

Theoretical biogas yield of 1.5 g cellulose = 1.5 * 830
= 1245 ml at STP

Phase 2: Sodium acetate (CH3COONa)

Two-step methanogenesis reaction:

$CH_3COO^- + H_2O \rightarrow 2HCO_3^- + 4H_2 + H^+$ (Syntrophic acetate oxidation)

$4H_2 + HCO_3^- + H^+ \rightarrow CH_4 + 3H_2O$ (Hydrogenotrophic methanogenesis)

Molecular weight of sodium acetate = 82 g/mol
Based on the equations, 1 mol acetate (CH_3COO^-) gives 1 mol methane.

Then, 2.28 g sodium acetate will give 2.28/82 = 0.0278 mol acetate
= 0.0278 mol methane

Using ideal gas law to get volume of methane at STP:

V = nRT/P
= 0.0278*8.314*273/101325
= 0.000623 m^3
= 623 ml

Assuming volume of produced methane and carbon dioxide to be in the ratio 50:50, theoretical biogas potential of 2.28 g sodium acetate = 2*623 = 1246 ml at STP

Appendix D

Table D1 shows the daily recorded pressure reading in each test reactor throughout the duration of the experiment.

Experiment phase	Days since start of experiment	Date of reading	Time of reading	Reactors at 55 °C									Reactors at room temp 21 °C		
				A1	A2	A3	B1	B2	B3	C1	C2	C3	E	D1	D2	D3
Start of Phase 1	0	22-02-2024	11:30:00	26.2	26.2	25.1	28.6	29	28.3	29.4	26.9	27	24.5	11	11	10.1
	1	23-02-2024	10:30:00	48.2	45.3	45.7	49.7	48.5	46.4	47.7	46.8	45.3	47.2	10.1	9.8	9.5
	3	25-02-2024	10:30:00	156.6	142.3	154.3	202.2	202.4	201.2	169.9	186	182.2	19.7	19.3	19.3	20.2
	4	26-02-2024	11:00:00	115.5	136	112.9	107.4	107.9	101.9	108.5	107.5	108.5	10.6	47.7	47.6	46.9
	5	27-02-2024	11:00:00	78.6	72.3	78.1	58.6	59.4	55.1	90.3	72.7	69.1	11.1	93.7	94.5	94.8
	6	28-02-2024	11:00:00	109.8	75.3	99	98.3	92.6	89.8	120.8	104.7	101.9	14.7	81.2	80.7	79.7
	7	29-02-2024	11:00:00	105.2	91.5	93	110.5	110.1	110	94.9	90.4	85	24.1	62.3	63.4	63.6
	8	01-03-2024	11:00:00	91.2	89.6	77.8	98.6	101.3	98.8	74.2	75.6	76.3	22	52.7	54	54.2
	10	03-03-2024	10:30:00	119.3	128.1	119.2	76.2	79.6	78.8	105.4	109.1	109.3	30.5	46.3	48.7	48.5
	11	04-03-2024	11:00:00	24.3	36.4	32.1	42	40.3	38.3	22.8	38.3	33.4	22.4	28.1	28.2	29
	12	05-03-2024	11:00:00	25.8	32.5	24.2	17.2	20.1	16.7	20	20.2	17.2	16.4	20.4	20.7	21.5
	13	06-03-2024	11:00:00	20.6	19	15	16.3	21.1	11.2	15	16.4	5.2	12	17.4	17.5	17.4
	14	07-03-2024	11:00:00	26.2	20	23.7	28.8	27.9	25.5	13	10.5	10.6	14.4	11	13	14.1
	15	08-03-2024	11:00:00	22.3	18.9	18.3	25.5	18.5	17	13.7	12.9	12.6	11.9	10	8.6	11.4
	18	11-03-2024	11:00:00	33.2	38.2	28.2	29.6	24.4	21.4	44.3	42.8	37.6	28.8	33.1	23.7	30.8
	19	12-03-2024	12:00:00	12.4	10	9.2	12.5	11	9.5	16.4	15.5	13.9	11.3	11.3	13.4	10.2
	20	13-03-2024	11:00:00	6.3	5.5	4.2	7.3	6.3	5.9	10.2	8.8	7.2	10.1	7.4	10.5	6.3
	21	14-03-2024	11:00:00	9.1	7.6	6.2	9	8.4	5.9	8.4	6.7	5.4	8.3	7.8	9.6	8
	22	15-03-2024	11:00:00	8.6	7	6	5	4.1	3.7	3.8	3.5	3	6.7	6.5	7.5	5.7
End of Phase 1 Start of Phase 2	25	18-03-2024	10:00:00	12.3	10.1	8.6	9.3	8.5	6.8	9.6	8.7	8.2	6.6	11	12.4	11.6
	26	19-03-2024	11:00:00	52	47.7	46.4	56.5	52.8	51.8	41.8	38.5	38.6	36.1	24.3	24.4	25.1
	27	20-03-2024	11:00:00	22.5	20.5	18.1	33.5	34.9	33.8	14.3	14.6	12.9	3.1	16.1	14.9	16.2
	28	21-03-2024	11:00:00	28.3	24.9	24	46.1	47.2	45.4	11.1	11.5	11	0	12.3	11.6	13.2
	29	22-03-2024	11:00:00	27.4	24.4	23.4	53.6	50.7	49.9	21.8	24.5	22.6	5.6	15.1	14.6	16.4
	31	24-03-2024	10:30:00	55	51.4	51.5	124	122	122.3	54.3	57	51	12.3	23.8	22.8	25.8
	32	25-03-2024	11:00:00	32.2	26.6	27.9	62.1	68.2	62.9	33.2	38.4	32	0	12.4	13.4	14.5
	33	26-03-2024	11:00:00	39.9	36	37.1	41.1	45.5	46.3	39.7	45.4	36.8	0	12.4	12.1	13.3
	34	27-03-2024	11:00:00	31.1	27.5	30.3	42.6	46.5	41.2	36.3	40.1	33.6	10.2	11.3	11.4	16
	35	28-03-2024	11:00:00	28.7	25.4	29.2	24.8	23.8	23.1	36.4	36.7	43.7	4.1	12.7	11.6	12.5
	40	02-04-2024	11:00:00	117.5	114.2	135.8	39.2	32.9	30.2	95.1	87.2	86.3	8.6	41.6	41.7	45.1
	41	03-04-2024	11:00:00	20.4	19.4	18.4	9.5	8	7.5	22.7	18.4	17.1	5	8.2	8.1	30.1
	42	04-04-2024	11:00:00	16.2	14.6	15.2	9.5	10	10.1	15.1	14.4	13	6	8.5	8.3	8.9
	43	05-04-2024	11:00:00	14.4	12.5	13.5	5.7	5.2	2.7	15.8	9.9	8.2	0	8.7	7.5	8.5
	46	08-04-2024	11:00:00	22.3	23.6	22.4	4	5.7	4.2	31.2	26.4	24.2	12.9	18.3	18.3	19.9
	47	09-04-2024	11:00:00	10.5	9.2	7.2	12.2	8.7	8.3	9	4.2	3.2	4.9	8.1	10.2	20.5
End of Phase 2	48	10-04-2024	11:00:00	0	0	0	0.4	0	0	0	0	0	0	5.6	5.8	6.6

Table D2 shows the calculated number of moles of produced biogas in each test reactor throughout the duration of the experiment.

Experiment phase	Days since start of experiment	Date	Reactors at 55 °C									Reactors at room temp 21 °C		
			A1	A2	A3	B1	B2	B3	C1	C2	C3	E1	D1	D2	D3
Start of Phase 1	0	22-02-2024	0.00166	0.00166	0.00159	0.00182	0.00184	0.00180	0.00187	0.00171	0.00171	0.00156	0.00078	0.00078	0.00072
	1	23-02-2024	0.00306	0.00288	0.00290	0.00316	0.00308	0.00295	0.00303	0.00297	0.00288	0.00300	0.00072	0.00069	0.00067
	3	25-02-2024	0.00995	0.00904	0.00980	0.01284	0.01286	0.01278	0.01079	0.01181	0.01157	0.00125	0.00137	0.00137	0.00143
	4	26-02-2024	0.00734	0.00864	0.00717	0.00682	0.00685	0.00647	0.00689	0.00683	0.00689	0.00067	0.00338	0.00337	0.00332
	5	27-02-2024	0.00499	0.00459	0.00496	0.00372	0.00377	0.00350	0.00574	0.00462	0.00439	0.00071	0.00664	0.00669	0.00671
	6	28-02-2024	0.00697	0.00478	0.00629	0.00624	0.00588	0.00570	0.00767	0.00665	0.00647	0.00093	0.00575	0.00572	0.00564
	7	29-02-2024	0.00668	0.00581	0.00591	0.00702	0.00699	0.00699	0.00603	0.00574	0.00540	0.00153	0.00441	0.00449	0.00450
	8	01-03-2024	0.00579	0.00569	0.00494	0.00626	0.00643	0.00628	0.00471	0.00480	0.00485	0.00140	0.00373	0.00382	0.00384
	10	03-03-2024	0.00758	0.00814	0.00757	0.00484	0.00506	0.00501	0.00669	0.00693	0.00694	0.00194	0.00328	0.00345	0.00344
	11	04-03-2024	0.00154	0.00231	0.00204	0.00267	0.00256	0.00243	0.00145	0.00243	0.00212	0.00142	0.00199	0.00200	0.00205
	12	05-03-2024	0.00164	0.00206	0.00154	0.00109	0.00128	0.00106	0.00127	0.00128	0.00109	0.00104	0.00144	0.00147	0.00152
	13	06-03-2024	0.00131	0.00121	0.00095	0.00104	0.00134	0.00071	0.00095	0.00104	0.00033	0.00076	0.00123	0.00124	0.00123
	14	07-03-2024	0.00166	0.00127	0.00151	0.00183	0.00177	0.00162	0.00083	0.00067	0.00067	0.00091	0.00078	0.00092	0.00100
	15	08-03-2024	0.00142	0.00120	0.00116	0.00162	0.00118	0.00108	0.00087	0.00082	0.00080	0.00076	0.00071	0.00061	0.00081
	18	11-03-2024	0.00211	0.00243	0.00179	0.00188	0.00155	0.00136	0.00281	0.00272	0.00239	0.00183	0.00234	0.00168	0.00218
	19	12-03-2024	0.00079	0.00064	0.00058	0.00079	0.00070	0.00060	0.00104	0.00098	0.00088	0.00072	0.00080	0.00095	0.00072
	20	13-03-2024	0.00040	0.00035	0.00027	0.00046	0.00040	0.00037	0.00065	0.00056	0.00046	0.00064	0.00052	0.00074	0.00045
	21	14-03-2024	0.00058	0.00048	0.00039	0.00057	0.00053	0.00037	0.00053	0.00043	0.00034	0.00053	0.00055	0.00068	0.00057
	22	15-03-2024	0.00055	0.00044	0.00038	0.00032	0.00026	0.00024	0.00024	0.00022	0.00019	0.00043	0.00046	0.00053	0.00040
End of Phase 1 Start of Phase 2	25	18-03-2024	0.00078	0.00064	0.00055	0.00059	0.00054	0.00043	0.00061	0.00055	0.00052	0.00042	0.00078	0.00088	0.00082
	26	19-03-2024	0.00330	0.00303	0.00295	0.00359	0.00335	0.00329	0.00266	0.00245	0.00245	0.00229	0.00172	0.00173	0.00178
	27	20-03-2024	0.00143	0.00130	0.00115	0.00213	0.00222	0.00215	0.00091	0.00093	0.00082	0.00020	0.00114	0.00106	0.00115
	28	21-03-2024	0.00180	0.00158	0.00152	0.00293	0.00300	0.00288	0.00071	0.00073	0.00070	0.00000	0.00087	0.00082	0.00093
	29	22-03-2024	0.00174	0.00155	0.00149	0.00340	0.00322	0.00317	0.00138	0.00156	0.00144	0.00036	0.00107	0.00103	0.00116
	31	24-03-2024	0.00349	0.00326	0.00327	0.00788	0.00775	0.00777	0.00345	0.00362	0.00324	0.00078	0.00169	0.00161	0.00183
	32	25-03-2024	0.00205	0.00169	0.00177	0.00394	0.00433	0.00400	0.00211	0.00244	0.00203	0.00000	0.00088	0.00095	0.00103
	33	26-03-2024	0.00253	0.00229	0.00236	0.00261	0.00289	0.00294	0.00252	0.00288	0.00234	0.00000	0.00088	0.00086	0.00094
	34	27-03-2024	0.00198	0.00175	0.00192	0.00271	0.00295	0.00262	0.00231	0.00255	0.00213	0.00065	0.00080	0.00081	0.00113
	35	28-03-2024	0.00182	0.00161	0.00185	0.00158	0.00151	0.00147	0.00231	0.00233	0.00278	0.00026	0.00090	0.00082	0.00089
	40	02-04-2024	0.00746	0.00725	0.00863	0.00249	0.00209	0.00192	0.00604	0.00554	0.00548	0.00055	0.00295	0.00295	0.00319
	41	03-04-2024	0.00130	0.00123	0.00117	0.00060	0.00051	0.00048	0.00144	0.00117	0.00109	0.00032	0.00058	0.00057	0.00213
	42	04-04-2024	0.00103	0.00093	0.00097	0.00060	0.00064	0.00064	0.00096	0.00091	0.00083	0.00038	0.00060	0.00059	0.00063
	43	05-04-2024	0.00091	0.00079	0.00086	0.00036	0.00033	0.00017	0.00100	0.00063	0.00052	0.00000	0.00062	0.00053	0.00060
	46	08-04-2024	0.00142	0.00150	0.00142	0.00025	0.00036	0.00027	0.00198	0.00168	0.00154	0.00082	0.00130	0.00130	0.00141
	47	09-04-2024	0.00067	0.00058	0.00046	0.00077	0.00055	0.00053	0.00057	0.00027	0.00020	0.00031	0.00057	0.00072	0.00145
End of Phase 2	48	10-04-2024	0.00000	0.00000	0.00000	0.00003	0.00000	0.00000	0.00000	0.00000	0.00000	0.00000	0.00040	0.00041	0.00047

Table D3 shows the produced biogas volume (in ml at STP) in each test reactor throughout the duration of the experiment.

Experiment phase	Days since start of experiment	Date	Reactors at 55 °C									Reactors at room temp 21 °C		
			A1	A2	A3	B1	B2	B3	C1	C2	C3	E1	D1	D2	D3
Start of Phase 1	0	22-02-2024	37.3	37.3	35.7	40.7	41.3	40.3	41.9	38.3	38.4	34.9	17.5	17.5	16.0
	1	23-02-2024	68.6	64.5	65.1	70.8	69.0	66.1	67.9	66.6	64.5	67.2	16.0	15.6	15.1
	3	25-02-2024	222.9	202.6	219.7	287.8	288.1	286.4	241.9	264.8	259.4	28.0	30.6	30.6	32.1
	4	26-02-2024	164.4	193.6	160.7	152.9	153.6	145.1	154.5	153.0	154.5	15.1	75.7	75.6	74.4
	5	27-02-2024	111.9	102.9	111.2	83.4	84.6	78.4	128.5	103.5	98.4	15.8	148.7	150.0	150.5
	6	28-02-2024	156.3	107.2	140.9	139.9	131.8	127.8	172.0	149.0	145.1	20.9	128.9	128.1	126.5
	7	29-02-2024	149.8	130.3	132.4	157.3	156.7	156.6	135.1	128.7	121.0	34.3	98.9	100.6	101.0
	8	01-03-2024	129.8	127.6	110.8	140.4	144.2	140.7	105.6	107.6	108.6	31.3	83.7	85.7	86.0
	10	03-03-2024	169.8	182.4	169.7	108.5	113.3	112.2	150.0	155.3	155.6	43.4	73.5	77.3	77.0
	11	04-03-2024	34.6	51.8	45.7	59.8	57.4	54.5	32.5	54.5	47.5	31.9	44.6	44.8	46.0
	12	05-03-2024	36.7	46.3	34.5	24.5	28.6	23.8	28.5	28.8	24.5	23.3	32.4	32.9	34.1
	13	06-03-2024	29.3	27.0	21.4	23.2	30.0	15.9	21.4	23.3	7.4	17.1	27.6	27.8	27.6
	14	07-03-2024	37.3	28.5	33.7	41.0	39.7	36.3	18.5	14.9	15.1	20.5	17.5	20.6	22.4
	15	08-03-2024	31.7	26.9	26.1	36.3	26.3	24.2	19.5	18.4	17.9	16.9	15.9	13.7	18.1
	18	11-03-2024	47.3	54.4	40.1	42.1	34.7	30.5	63.1	60.9	53.5	41.0	52.5	37.6	48.9
	19	12-03-2024	17.7	14.2	13.1	17.8	15.7	13.5	23.3	22.1	19.8	16.1	17.9	21.3	16.2
	20	13-03-2024	9.0	7.8	6.0	10.4	9.0	8.4	14.5	12.5	10.2	14.4	11.7	16.7	10.0
	21	14-03-2024	13.0	10.8	8.8	12.8	12.0	8.4	12.0	9.5	7.7	11.8	12.4	15.2	12.7
	22	15-03-2024	12.2	10.0	8.5	7.1	5.8	5.3	5.4	5.0	4.3	9.5	10.3	11.9	9.0
End of Phase 1 Start of Phase 2	25	18-03-2024	17.5	14.4	12.2	13.2	12.1	9.7	13.7	12.4	11.7	9.4	17.5	19.7	18.4
	26	19-03-2024	74.0	67.9	66.1	80.4	75.2	73.7	59.5	54.8	55.0	51.4	38.6	38.7	39.8
	27	20-03-2024	32.0	29.2	25.8	47.7	49.7	48.1	20.4	20.8	18.4	4.4	25.6	23.7	25.7
	28	21-03-2024	40.3	35.4	34.2	65.6	67.2	64.6	15.8	16.4	15.7	0.0	19.5	18.4	21.0
	29	22-03-2024	39.0	34.7	33.3	76.3	72.2	71.0	31.0	34.9	32.2	8.0	24.0	23.2	26.0
	31	24-03-2024	78.3	73.2	73.3	176.5	173.7	174.1	77.3	81.1	72.6	17.5	37.8	36.2	41.0
	32	25-03-2024	45.8	37.9	39.7	88.4	97.1	89.5	47.3	54.7	45.6	0.0	19.7	21.3	23.0
	33	26-03-2024	56.8	51.2	52.8	58.5	64.8	65.9	56.5	64.6	52.4	0.0	19.7	19.2	21.1
	34	27-03-2024	44.3	39.1	43.1	60.6	66.2	58.7	51.7	57.1	47.8	14.5	17.9	18.1	25.4
	35	28-03-2024	40.9	36.2	41.6	35.3	33.9	32.9	51.8	52.2	62.2	5.8	20.2	18.4	19.8
	40	02-04-2024	167.3	162.6	193.3	55.8	46.8	43.0	135.4	124.1	122.9	12.2	66.0	66.2	71.6
	41	03-04-2024	29.0	27.6	26.2	13.5	11.4	10.7	32.3	26.2	24.3	7.1	13.0	12.9	47.8
	42	04-04-2024	23.1	20.8	21.6	13.5	14.2	14.4	21.5	20.5	18.5	8.5	13.5	13.2	14.1
	43	05-04-2024	20.5	17.8	19.2	8.1	7.4	3.8	22.5	14.1	11.7	0.0	13.8	11.9	13.5
	46	08-04-2024	31.7	33.6	31.9	5.7	8.1	6.0	44.4	37.6	34.5	18.4	29.0	29.0	31.6
	47	09-04-2024	14.9	13.1	10.2	17.4	12.4	11.8	12.8	6.0	4.6	7.0	12.9	16.2	32.5
End of Phase 2	48	10-04-2024	0.0	0.0	0.0	0.6	0.0	0.0	0.0	0.0	0.0	0.0	8.9	9.2	10.5

Table D4 shows the average value of produced biogas volume (in ml at STP) with standard deviation for each reactor group.

iment phase	Days since start of experiment	A_mean	A_sd	B_mean	B_sd	C_mean	C_sd	D_mean	D_sd	E	
Start of Phase 1	0	36.78	0.74	40.76	0.41	39.53	1.65	16.99	0.67	34.88	
	1	66.05	1.83	68.62	1.94	66.34	1.41	15.56	0.39	67.19	
	3	215.06	8.93	287.47	0.75	255.34	9.78	31.11	0.67	28.04	
	4	172.92	14.71	150.52	3.87	153.98	0.67	75.24	0.56	15.09	
	5	108.67	4.07	82.14	2.66	110.14	13.19	149.75	0.74	15.80	
	6	134.81	20.51	133.20	5.03	155.36	11.86	127.84	0.99	20.93	
	7	137.47	8.73	156.88	0.31	128.27	5.76	100.17	0.91	34.31	
	8	122.71	8.51	141.74	1.75	107.29	1.24	85.14	1.06	31.32	
	10	173.96	5.94	111.32	2.07	153.65	2.55	75.93	1.73	43.42	
	11	44.04	7.13	57.23	2.15	44.84	9.21	45.14	0.64	31.89	
	12	39.15	5.12	25.62	2.13	27.24	1.95	33.12	0.74	23.35	
	13	25.91	3.35	23.06	5.75	17.37	7.09	27.67	0.07	17.08	
	14	33.17	3.63	39.01	1.98	16.18	1.65	20.16	2.04	20.50	
	15	28.23	2.51	28.95	5.27	18.60	0.66	15.87	1.81	16.94	
	18	47.26	5.81	35.78	4.82	59.17	4.09	46.35	6.35	41.00	
	19	15.00	1.94	15.66	1.74	21.73	1.47	18.47	2.11	16.09	
	20	7.59	1.23	9.25	0.84	12.43	1.74	12.81	2.82	14.38	
	21	10.87	1.69	11.06	1.91	9.73	1.75	13.44	1.28	11.82	
	22	10.25	1.52	6.07	0.77	4.89	0.47	10.42	1.17	9.54	
End of Phase 1 Start of Phase 2	25	14.71	2.16	11.67	1.48	12.58	0.82	18.52	0.91	9.40	
	26	69.33	3.41	76.45	2.88	56.42	2.18	39.05	0.56	51.39	
	27	28.99	2.56	48.50	0.86	19.84	1.05	24.98	0.94	4.41	
	28	36.63	2.64	65.82	1.05	15.94	0.31	19.63	1.04	0.00	
	29	35.68	2.42	73.17	2.26	32.70	1.61	24.39	1.20	7.97	
	31	74.93	2.38	174.77	1.25	77.02	3.49	38.31	1.98	17.51	
	32	41.14	3.41	91.68	3.85	49.16	3.95	21.32	1.36	0.00	
	33	53.62	2.34	63.06	3.25	57.85	5.09	20.00	0.81	0.00	
	34	42.19	2.20	61.83	3.19	52.20	3.80	20.48	3.48	14.52	
	35	39.53	2.40	34.02	0.99	55.42	4.80	19.47	0.76	5.84	
	40	174.39	13.52	48.54	5.37	127.46	5.63	67.94	2.58	12.24	
	41	27.62	1.16	11.86	1.21	27.62	3.41	24.55	16.43	7.12	
	42	21.83	0.94	14.05	0.37	20.17	1.24	13.60	0.40	8.54	
	43	19.17	1.10	6.45	1.87	16.09	4.64	13.07	0.83	0.00	
	46	32.41	0.84	6.60	1.08	38.82	4.16	29.90	1.20	18.36	
	47	12.76	1.93	13.86	2.49	7.78	3.60	20.53	8.60	6.98	
End of Phase 2	48	0.00	0.00	0.19	0.27	0.00	0.00	9.52	0.69	0.00	

Table D5 shows the average cumulative biogas production (in ml at STP) with standard deviation for each reactor group.

Experiment phase	Days since start of experiment	A_mean	A_sd	B_mean	B_sd	C_mean	C_sd	D_mean	D_sd	E
Start of Phase 1	0	36.78	0.74	40.76	0.41	39.53	1.65	16.99	0.67	34.88
	1	102.83	1.83	109.38	1.94	105.87	1.41	32.54	0.39	102.07
	3	317.89	8.93	396.85	0.75	361.21	9.78	63.66	0.67	130.12
	4	490.81	14.71	547.37	3.87	515.20	0.67	138.90	0.56	145.21
	5	599.47	4.07	629.51	2.66	625.33	13.19	288.64	0.74	161.01
	6	734.29	20.51	762.71	5.03	780.69	11.86	416.48	0.99	181.93
	7	871.76	8.73	919.59	0.31	908.96	5.76	516.65	0.91	216.24
	8	994.47	8.51	1061.33	1.75	1016.25	1.24	601.79	1.06	247.56
	10	1168.43	5.94	1172.66	2.07	1169.90	2.55	677.72	1.73	290.98
	11	1212.47	7.13	1229.88	2.15	1214.75	9.21	722.85	0.64	322.87
	12	1251.62	5.12	1255.51	2.13	1241.98	1.95	755.98	0.74	346.22
	13	1277.53	3.35	1278.57	5.75	1259.35	7.09	783.65	0.07	363.30
	14	1310.70	3.63	1317.58	1.98	1275.53	1.65	803.81	2.04	383.80
	15	1338.93	2.51	1346.52	5.27	1294.13	0.66	819.68	1.81	400.74
	18	1386.19	5.81	1382.30	4.82	1353.31	4.09	866.04	6.35	441.74
	19	1401.19	1.94	1397.96	1.74	1375.04	1.47	884.50	2.11	457.83
	20	1408.78	1.23	1407.21	0.84	1387.47	1.74	897.31	2.82	472.20
	21	1419.65	1.69	1418.27	1.91	1397.20	1.75	910.75	1.28	484.02
	22	1429.90	1.52	1424.35	0.77	1402.09	0.47	921.17	1.17	493.56
End of Phase 1 Start of Phase 2	25	1444.61	2.16	1436.02	1.48	1414.66	0.82	939.69	0.91	502.95
	26	1513.94	3.41	1512.47	2.88	1471.09	2.18	978.74	0.56	554.34
	27	1542.93	2.56	1560.96	0.86	1490.92	1.05	1003.72	0.94	558.76
	28	1579.56	2.64	1626.78	1.05	1506.87	0.31	1023.35	1.04	558.76
	29	1615.25	2.42	1699.95	2.26	1539.56	1.61	1047.74	1.20	566.73
	31	1690.18	2.38	1874.72	1.25	1616.58	3.49	1086.05	1.98	584.24
	32	1731.32	3.41	1966.40	3.85	1665.74	3.95	1107.38	1.36	584.24
	33	1784.94	2.34	2029.46	3.25	1723.58	5.09	1127.38	0.81	584.24
	34	1827.13	2.20	2091.30	3.19	1775.78	3.80	1147.86	3.48	598.76
	35	1866.65	2.40	2125.32	0.99	1831.21	4.80	1167.33	0.76	604.60
	40	2041.04	13.52	2173.86	5.37	1958.66	5.63	1235.27	2.58	616.84
	41	2068.66	1.16	2185.73	1.21	1986.28	3.41	1259.82	16.43	623.96
	42	2090.49	0.94	2199.77	0.37	2006.45	1.24	1273.42	0.40	632.50
	43	2109.66	1.10	2206.23	1.87	2022.54	4.64	1286.49	0.83	632.50
	46	2142.07	0.84	2212.82	1.08	2061.35	4.16	1316.38	1.20	650.86
	47	2154.83	1.93	2226.68	2.49	2069.13	3.60	1336.92	8.60	657.84
End of Phase 2	48	2154.83	0.00	2226.87	0.27	2069.13	0.00	1346.44	0.69	657.84

DEPARTMENT OF ARCHITECTURE AND CIVIL ENGINEERING
CHALMERS UNIVERSITY OF TECHNOLOGY
Gothenburg, Sweden 2024

CHALMERS
UNIVERSITY OF TECHNOLOGY